Silsesquioxane Models for Silica Surface Silanol Sites with Adjacent Siloxide Functionalites and Olefin Polymerization Catalysts Thereof

Robbert Duchateau,*[a] Tessa W. Dijkstra,[b] Rutger A. van Santen,[b] and Glenn P. A. Yap[c]

Abstract: Incompletely condensed silsesquioxanes of the type $R_7Si_7O_9(O\{SiR'_2O\}_n)OH$ ($R = c\text{-}C_5H_9$, $c\text{-}C_6H_{11}$; $R' = Me$, Ph; $n = 1–4$), containing a siloxane ring of variable size and rigidity and a remaining silanol, are described. Compared with a truly isolated silanol $[R_7Si_8O_{12}(OH)]$, solution and solid state FT-IR spectra of these compounds show a $\tilde{\nu}_{OH}$ shift of approximately 150 cm^{-1} to lower frequency, which suggests hydrogen bonding of the silanol with the internal siloxane ring. In agreement with this, the relative ion pair acidities of the silanols in THF, determined by UV/Vis, were lowered by 0.8–1.2 compared with a truly isolated silanol. Density functional theory (DFT) calculations on these systems confirm the presence of intramolecular hydrogen bonding. Possible interaction of the silyl ether functionalities with Lewis acidic metal sites was studied for the neutral gallium-substituted systems and cationic titanium silsesquioxane complexes, models for an immobilized titanium olefin polymerization catalyst. The electron donating capability of the siloxide functionalities in **1**, **6**, and **7** is not sufficient to satisfy the electron deficiency of the corresponding gallium silsesquioxane species, which form dimeric structures with a bridging siloxide unit rather than Lewis base adducts with coordinated siloxide functionalities. Metallation of **1** and **4** with $[Cp''Ti(CH_2Ph)_3]$ ($Cp'' = \eta^5\text{-}1,3\text{-}C_5H_3(SiMe_3)_2$) in a 1:1 ratio afforded monomeric titanasilsesquioxanes. To probe the effect of the neighboring siloxane ring on the highly Lewis acidic titanium center, the catalytic activities of the corresponding cationic half-sandwich complexes were tested in 1-hexene polymerization. Compared with the catalyst system based on the isolated silanol $[(c\text{-}C_5H_9)_7Si_8O_{12}OH]$, the presence of a neighboring siloxane ring causes considerable retardation of the polymerization process but also improves the stability of the catalyst.

Keywords: polymerization • silicon • silsesquioxanes • titanium

Introduction

Amorphous silicas play an important role in many different disciplines of chemistry. Silicious materials are used, for example, as absorbents and fillers, in acid-catalyzed reactions, or as catalyst supports.[1–4] The properties of silicas are strongly affected by the nature and number of their surface silanols, which can effectively be varied using different calcination conditions. The silica surface silanols can react with various organic and inorganic substrates, which makes it possible to change the properties of the silica.[1–2] This makes silica one of the most frequently used support materials for immobilizing homogeneous catalysts.

At present, there is considerable interest in the immobilization of well-defined homogeneous olefin polymerization catalysts.[4] The goal is to marry the advantages of homogeneous and heterogeneous systems. Homogeneous catalysts are well-defined, single-site catalysts that can be fine-tuned to produce tailor-made polymers. Heterogeneous catalysts, however, have the technologic advantages of good morphology control, high polymer bulk density, and lack of reactor fouling. Since most of the existing polymerization plants run reactions as slurry or gas-phase processes with heterogeneous catalyst, homogeneous catalysts must be heterogenized on a support to be used in these processes. One of the earliest and most studied methods for immobilization of the catalyst system consists of grafting homogeneous catalyst precursors onto silica supports.[5] Thorough studies by Basset

---

[a] Dr. R. Duchateau
Department of Polymer Chemistry
Eindhoven University of Technology
PO Box 513, 5600 MB Eindhoven (The Netherlands)
Fax: (+31) 40-246-3966
E-mail: R.Duchateau@tue.nl

[b] Dr. T. W. Dijkstra, Prof. Dr. R. A. van Santen
Department of Inorganic Chemistry and Catalysis
Eindhoven University of Technology
PO Box 513, 5600 MB Eindhoven (The Netherlands)

[c] Dr. G. P. A. Yap
Chemistry Department, University of Ottawa
K1N 6N5 Ottawa, Ontario (Canada)

DOI: 10.1002/chem.200400206

and Marks on [Cp*$ZrMe_3$] supported on silica and sulfated zirconia, respectively, has given insight into the structure of the surface sites.[6] Whereas these supported systems showed significant catalytic activity, direct grafting of catalyst precursors onto oxidic supports is often accompanied by dramatic reduction of catalyst activity. The inhomogeneity of the support forms an explanation for this deactivation. Interaction of the supported catalysts with adjacent hydroxyl or siloxide groups is believed to poison a major portion of the catalytic sites. Clearly, the heterogeneous nature of real supports makes studying such interactions very difficult.

The silicalite cage structures of incompletely condensed silsesquioxanes with formula $(RSiO_{3/2})_n$ show striking similarities to known morphologies of silica and have proven over the years to be one of the most realistic homogeneous models for both silica surfaces and zeolites.[7,8] A hydrophobic coat of alkyl groups bound to the corners of the silicate cages make the molecules soluble in organic solvents and enables investigation on a molecular level with a wide range of powerful techniques such as multinuclear solution NMR spectroscopy and single X-ray diffraction. Modifying the acidity and reactivity of silica surfaces, for example, by silylation, can be modeled and studied in detail with silsesquioxanes. Starting from the most widely used incompletely condensed silsesquioxanes $[R_7Si_7O_9(OH)_3]$ (R = c-C_5H_9, c-C_6H_{11}) several silylation reactions have been studied, affording various types of silanol sites: vicinal silanols (hydrogen-bonded silanols), geminal silanols (two hydroxyls attached to the same silicon atom)[4] and isolated silanols.[7] In the past, silsesquioxanes have also successfully been used to model various silica-grafted olefin polymerization (co)catalysts such as Group 13 element doped silicas, silica-grafted perfluoroborato cocatalysts, surface-supported (half-) metallocenes and organometallic complexes, and traditional heterogeneous (Ziegler–Natta and Phillips type) olefin polymerization catalysts.[8] However, the possible effect of neighboring silanols or siloxides on the catalyst performance has never been studied using silsesquioxane model systems.

We were interested in studying the possible interaction of adjacent siloxide functionalities with Lewis acidic metal sites in silica-supported catalysts. For this study, we prepared silsesquioxane monosilanols with an adjacent siloxane ring of variable size, obtained from the reaction of $[R_7Si_7O_9(OH)_3]$ (R = c-C_5H_9, c-C_6H_{11}) and several dichlorosil(ox)anes. First, the influence of the neighboring siloxane ring on the hydrogen-bonding ability and acidity of the silanol was investigated using NMR spectroscopy, IR spectroscopy, and DFT calculations. Possible interaction of the siloxide functionalities with Lewis acidic metal sites was studied for the neutral gallium-substituted systems and cationic titanium silsesquioxane complexes, which serve as a model for a silica-grafted titanium olefin polymerization catalyst.

Results and Discussion

Synthesis of disilylated silsesquioxanes 1–7: Treatment of $[(c\text{-}C_5H_9)_7Si_7O_9(OH)_3]$ with 0.95 equivalents of Cl_2SiMe_2 in the presence of NEt_3 in THF (stirred at room temperature overnight) selectively afforded the disilylated $[(c\text{-}C_5H_9)_7Si_7O_9(OSiMe_2O)OH]$ **1**. In the same manner, a variety of disilylated silsesquioxanes could be obtained from the reaction of $[R_7Si_7O_9(OH)_3]$ (R = c-C_5H_9, c-C_6H_{11}) with the dichlorosil(ox)anes $[ClSiMe_2\{OSiMe_2\}_nCl]$ (n = 0–3), Cl_2SiPh_2, and $[ClSiPh_2OSiPh_2Cl]$. Of the twelve possible products, seven products could actually be isolated in analytically pure form; $[(c\text{-}C_5H_9)_7Si_7O_9(OSiMe_2O)OH]$ **1**, $[(c\text{-}C_5H_9)_7Si_7O_9(O\{SiMe_2O\}_3)OH]$ **2**, $[(c\text{-}C_5H_9)_7Si_7O_9(O\{SiMe_2O\}_4)OH]$ **3**, $[(c\text{-}C_6H_{11})_7Si_7O_9(O\{SiMe_2O\}_2)OH]$ **4**, $[(c\text{-}C_6H_{11})_7Si_7O_9(O\{SiMe_2O\}_3)OH]$ **5**, $[(c\text{-}C_6H_{11})_7Si_7O_9(O\{SiMe_2O\}_4)OH]$ **6** and $[(c\text{-}C_5H_9)_7Si_7O(OSiPh_2O)OH]$ **7** (Scheme 1).

Interestingly, in some cases, the cyclopentyl-substituted silsesquioxane showed considerably different reactivity than the cyclohexyl-substituted analogue. Differences in reactivity between cyclopentyl- and cyclohexyl-substituted silsesquioxanes have been observed before, although the reason for this sometimes striking difference is still a puzzle.[9] Whereas reaction of Cl_2SiMe_2 and Cl_2SiPh_2 with cyclopentyl-substituted silsesquioxane $[(c\text{-}C_5H_9)_7Si_7O_9(OH)_3]$ selectively gave the products **1** and **7**, the same reaction with the cyclohexyl-substituted silsesquioxane $[(c\text{-}C_6H_{11})_7Si_7O_9(OH)_3]$ gave ill-defined mixtures. Only the reaction of $[(c\text{-}C_6H_{11})_7Si_7O_9(OH)_3]$ with 1.5 equivalents of Cl_2SiMe_2 resulted in a well-defined product, $\{(c\text{-}C_6H_{11})_7Si_7O_9(O_2SiMe_2)\}_2\{(\mu\text{-}O)_2SiMe_2\}$, as earlier reported by Edelmann et al.[10] In addition, the reaction with $[ClSiMe_2OSiMe_2Cl]$ was different for cyclohexyl and cyclopentyl-substituted trisilanols. In the case of the cyclohexyl-substituted silsesquioxane $[(c\text{-}C_6H_{11})_7Si_7O_9(OH)_3]$, a clean monomeric product $[(c\text{-}C_6H_{11})_7Si_7O_9(O\{SiMe_2O\}_2)OH]$ **4** could be obtained, whereas for the cyclopentyl analogue all efforts ended in unidentifiable mixtures. Disilylation of the trisilanols with longer methyl-substituted dichlorosilanes $[Cl(SiMe_2O)_nSiMe_2Cl]$ (n = 2, 3) in the presence of amine were straightforward. The reaction needed somewhat more forcing conditions (moderate heating for one night) but the expected products **2**, **3**, **5**, and **6** could be isolated in pure form for both cyclopentyl- and cyclohexyl-substituted silsesquioxanes. Reaction of $[ClSiPh_2OSiPh_2Cl]$ afforded ill-defined products for both $[(c\text{-}C_5H_9)_7Si_7O_9(OH)_3]$ and $[(c\text{-}C_6H_{11})_7Si_7O_9(OH)_3]$.

Identification of disilylated silsesquioxanes 1–7—Solution NMR spectroscopy: The ^{13}C and ^{29}Si NMR spectra of **1**–**7** show five CH-C_5H_9 and five $(-O)_3SiC_5H_9$ resonances, respectively in a 1:1:1:2:2 ratio, from which it can be concluded that compounds **1**–**7** show C_s symmetry. A selection of ^1H, ^{13}C, and ^{29}Si NMR data are shown in Table 1. The $SiMe_2$ methyl groups of product **4**, which has a siloxane ring with five silicon atoms (of which two are -$OSiMe_2$- units), give rise to two singlets in the ^1H and ^{13}C NMR spectra, which are assigned to two sets of inequivalent methyl groups. Products **2** and **5**, with a siloxane ring with six silicon atoms (of which three are -$OSiMe_2$- units), show four signals assigned to the six methyl groups in a 1:2:2:1 ratio in the ^1H NMR and ^{13}C NMR spectra. The ^{29}Si NMR spectra of **2** and **5** display two SiMe$_2$ resonances in a 1:2 ratio. Products **3** and **6**, with a siloxane ring of seven silicon atoms (of which

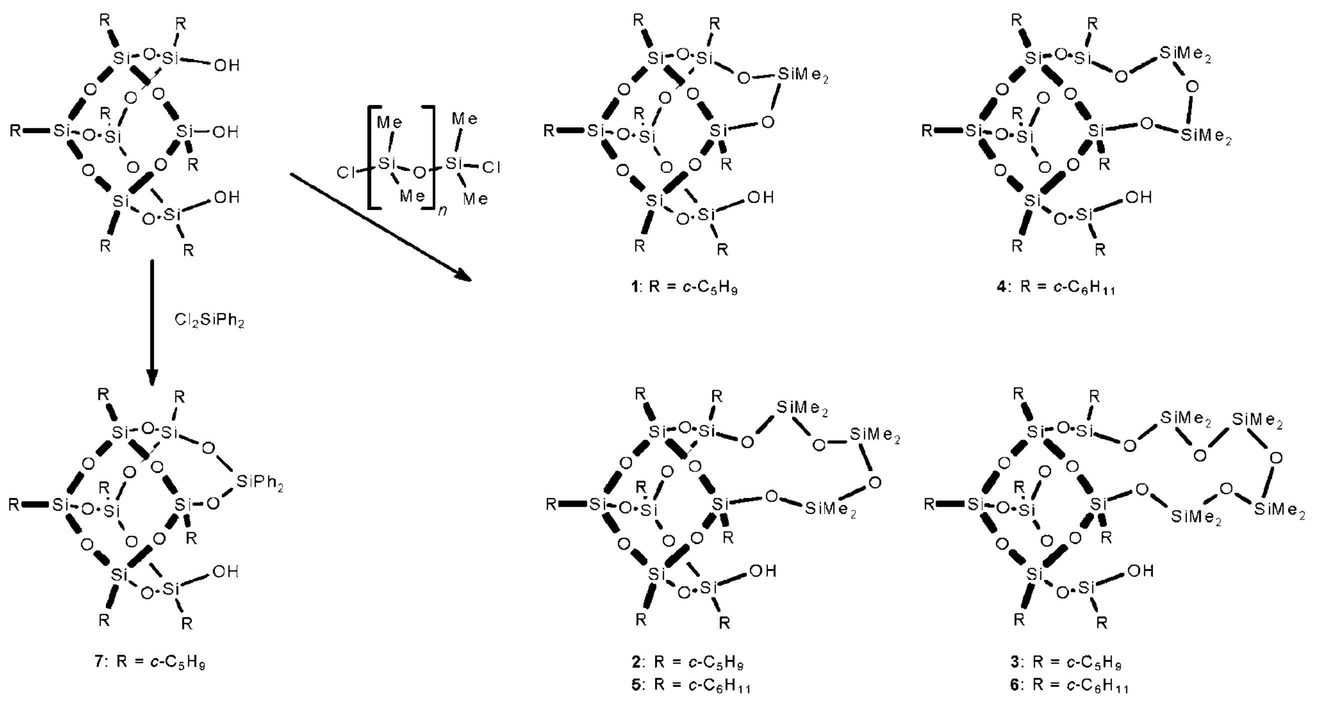

Scheme 1. Synthesis of incompletely condensed silsesquioxanes with methyl (**1**–**6**) or phenyl (**7**) substituted dichlorosilanes.

Table 1. Selected ^{1}H, ^{13}C, and ^{29}Si NMR data of **1**–**7**.

	SiO*H*, ^{1}H, CDCl$_3$ (C$_6$D$_6$)	Si(C*H*$_3$)$_2$ ^{1}H, CDCl$_3$ (ratio)	Si(*C*H$_3$)$_2$, ^{13}C, CDCl$_3$ (ratio)	***Si***OH, ^{29}Si, CDCl$_3$ (C$_6$D$_6$)	O$_2$***Si***R$_2$, ^{29}Si, CDCl$_3$ (ratio)
1	3.16 (3.38)	0.21, 0.23	0.04, 0.73	−56.04 (−55.39)	−16.02
2	3.91 (4.17)	0.14, 0.18, 0.19, 0.23 (1:2:2:1)	0.52, 0.70, 0.82, 0.91 (1:2:2:1)	−59.27 (−58.63	−17.68; −19.74 (1:2)
3	3.64 (3.78)	0.14, 0.17, 0.19 (1:2:1)	0.83, 0.98, 1.09 (1:2:1)	−58.95 (−58.40)	−20.27; −21.07 (1:1)
4	3.59 (3.98)	0.19, 0.20 (1:1)	0.43, 0.93 (1:1)	−60.32 (−59.46)	−17.92
5	3.94 (4.22)	0.13, 0.18, 0.21 (1:4:1)	0.56, 0.68, 0.85, 0.96 (1:2:2:1)	−61.53 (−60.85)	−17.50; −19.68 (1:2)
6	3.47 (3.84)	0.13, 0.15, 0.17, 0.18 (1:1:1:1)	0.86, 0.97, 1.06, 1.17 (1:1:1:1)	−61.13 (−60.39)	−20.15; −21.13 (1:1)
7	2.39 (2.73)	–	–	−58.07 (−57.82)	−46.69

four are -OSiMe$_2$- units), show three SiMe$_2$ methyl resonances in the ^{1}H and ^{13}C NMR spectra in a 1:2:1 ratio for **3** and four equally intense resonances for **6**. The ^{29}Si NMR spectra show two equally intense *Si*Me$_2$ resonances for both **3** and **6**. The proton resonances of the silanol groups in **1**–**6** are considerably shifted to lower field compared to the resonance of truly isolated silanols, which can be found at $\delta = 2.53$ for [(c-C$_5$H$_9$)$_7$Si$_8$O$_{12}$OH], $\delta = 2.49$ for [(c-C$_6$H$_{11}$)$_7$Si$_8$O$_{12}$(OH)], and $\delta = 2.79$ for [(c-C$_6$H$_{11}$)$_7$Si$_7$O$_9$(OSiMe$_3$)$_2$OH].[7g,h] The downfield shift for **1**–**6** can be explained by hydrogen bonding of the silanol with the adjacent siloxane ring. Truly isolated silanols only show some intermolecular hydrogen bonding. This is supported by the fact that ons going from [D]chloroform ($\varepsilon_{(20°C)} = 4.3$) to a less polar solvent such as [D$_6$]benzene ($\varepsilon_{(20°C)} = 2.3$), the proton signals of the perturbed silanols of compounds **1**–**6** are shifted towards lower field by an average of 0.3 ppm (Table 1). This indicates that when interactions of the silanols of compounds **1**–**6** with the solvent are decreased, intramolecular hydrogen bonding with the adjacent siloxide oxygens becomes stronger. For the unperturbed silanols, less interaction of the silanol with its medium results in a shift towards higher field. Hence, when going from CDCl$_3$ to [D$_6$]benzene as a solvent, compounds with unperturbed silanols shift towards higher field by more than 0.4 ppm in the ^{1}H spectra. The ^{1}H NMR spectrum (CDCl$_3$) of **7** shows an OH resonance at $\delta = 2.39$, which suggests that no hydrogen bonding is present in **7**. However, an additive shielding effect of the adjacent phenyl groups cannot be excluded.

Identification of disilylated silsesquioxanes 1–7—FT-IR spectroscopy: Infrared spectroscopy is a technique frequently used to study bulk properties of silica surfaces.[11] The OH stretching vibration of silanol groups in particular offers a great deal of information, for example on the process of dehydroxylation or dehydration of physisorbed water.[1] Krijnen and Harmsen successfully used FTIR data and DFT calculations of incompletely condensed silsesquioxanes as references for FT-IR assignments of hydroxyl clusters in zeolite structures.[9a,12] Here, attention will be focused on OH stretching vibrations of isolated silanols with and without the presence of an additional siloxide functionality. A full comparison of silsesquioxanes bearing different types of silanols with surface silanols is published elsewhere.[7g,h]

The infrared spectra of compounds **1**–**7** were examined both in solution (0.1 M in CCl_4) and in the solid state (Table 2). Solid-state spectra were recorded using Nujol mulls. On silica surfaces, a broad vibration band with a maximum near 3550 cm^{-1} is assigned to hydrogen-bonded silanol groups. After extensive thermal treatment a narrow band at 3750 cm^{-1} remains, which is assigned to truly isolated silanols. This agrees well with the sharp band around 3700 cm^{-1} found both in solution and in the solid state in the FTIR spectra of $[(c\text{-}C_5H_9)_7Si_8O_{12}(OH)]$.[7f–h] Also for other compounds containing isolated silanols, sharp bands in the same region have been observed (Table 2). In the solid-state IR spectrum of $[(c\text{-}C_5H_9)_7Si_8O_{12}(OH)]$, a second vibration band was observed at 3444 cm^{-1}, which was assigned to an intermolecular hydrogen bond of dimeric $\{(c\text{-}C_5H_9)_7Si_8O_{12}(\mu\text{-}OH)\}_2$, present in the crystalline phase. Compounds **1**–**7** show $\tilde{\nu}_{OH}$ frequencies in both solution and solid states, around 3550 cm^{-1} for the methyl-substituted compounds **1**–**6**, and at approximately 3635 cm^{-1} for the phenyl-substituted compound **7** (Table 2). Compounds **1**–**6**, containing flexible methyl-substituted siloxane rings, show broad stretching vibration bands at frequencies indicative of the presence of hydrogen bonding. To further study the possibility of intramolecular hydrogen bonding in **1**–**6**, the molecular structures of the models $H_7Si_7(O\{SiH_2O\}_n)OH$ (n = 1–4) were optimized using DFT calculations. For computational reasons, hydrogen atoms replace the silsesquioxane alkyl groups in these calculations. Although even small differences in steric bulk were found to have a significant influence on the structure of the complex, this approximation seems reasonable for the computation of an internal feature such as an intramolecular hydrogen bond. Intramolecular hydrogen bonding was observed in all the optimized structures (Figure 1). With $OH_2SiO\cdots O(H)Si$ distances ranging from 2.909 (**A**, Figure 1) to 2.836 Å (**D**, Figure 1), one oxygen of the $O(SiH_2O)_n$ groups is clearly bent towards the adjacent silanol, enabling the formation of a hydrogen bond. In these sterically unhindered hydrogen-substituted structures, the hydrogen bond strength increases with increasing siloxane ring size. The longer siloxane rings are more flexible and can more easily bend toward the silanol group. Strain in the smallest ring in **A** clearly hampers effective hydrogen bonding, which is in agreement with the observed large shift of the $\tilde{\nu}_{OH}$ frequency in the IR spectrum of **1** upon addition of a proton acceptor (see below). The $\tilde{\nu}_{OH}$ vibration band of the phenyl-substituted compound **7** is much narrower than for compounds **1**–**6** and its position (3635 cm^{-1}) suggests the presence of almost truly isolated silanols. The bulky phenyl groups of **7** probably complicate interaction of the silanol with the siloxide functionalities, unlike the methyl groups of **1**–**6**.

Table 2. FT-IR values in Nujol and CCl_4, estimated pK_{ip}* values and $\Delta\tilde{\nu}_{OH}$ FTIR values due to an external proton acceptor for **1**–**7** and $(c\text{-}C_5H_9)_7Si_8O_{12}(OH)$.

Compound	IR (Nujol mull) $\tilde{\nu}_{OH}$ [cm^{-1}]	IR (CCl_4) $\tilde{\nu}_{OH}$ [cm^{-1}]	IR ($CCl_4 + Et_2O$)[a] $\Delta\tilde{\nu}_{OH}$ [cm^{-1}]	pK_{ip}[b] (THF)
$(c\text{-}C_5H_9)_7Si_7O_9(O\{SiMe_2O\})OH$ (**1**)	3564	(3699), 3549	132	9.6 ± 0.4
$(c\text{-}C_5H_9)_7Si_7O_9(O\{SiMe_2O\}_3)OH$ (**2**)	3561	3594, 3511	49	10.5 ± 0.1
$(c\text{-}C_5H_9)_7Si_7O_9(O\{SiMe_2O\}_4)OH$ (**3**)	3606	3602, 3481	113	10.1 ± 0.1
$(c\text{-}C_6H_{11})_7Si_7O_9(O\{SiMe_2O\}_2)OH$ (**4**)	3561	3550	16	10.7 ± 0.3
$(c\text{-}C_6H_{11})_7Si_7O_9(O\{SiMe_2O\}_3)OH$ (**5**)	3598, 3516	3602, 3519	40	10.8 ± 0.1
$(c\text{-}C_6H_{11})_7Si_7O_9(O\{SiMe_2O\}_4)OH$ (**6**)	3668	3620, 3473	102	9.7 ± 0.3
$(c\text{-}C_5H_9)_7Si_7O_9(O\{SiPh_2O\})OH$ (**7**)	3661	3635	251	11.1 ± 0.4
$(c\text{-}C_5H_9)_7Si_8O_{12}OH$	3706, 3444	3700	359	8.9 ± 0.4

[a] Low frequency shift compared with $\tilde{\nu}(OH)$ value in neat CCl_4. [b] Relative ion-pair acidities pK_{ip}; averages of two indicators, $Li^+[9\text{-(cyano)fluorenide}]^-\cdot 2THF$ and $Li^+[9\text{-methoxycarbonyl)fluorenide}]^-\cdot 2THF$.

Identification of disilylated silsesquioxanes 1–7—Brønsted acidities: Although the overall Brønsted acidity of silica surface silanols is usually fairly weak, the differences in Brønst-

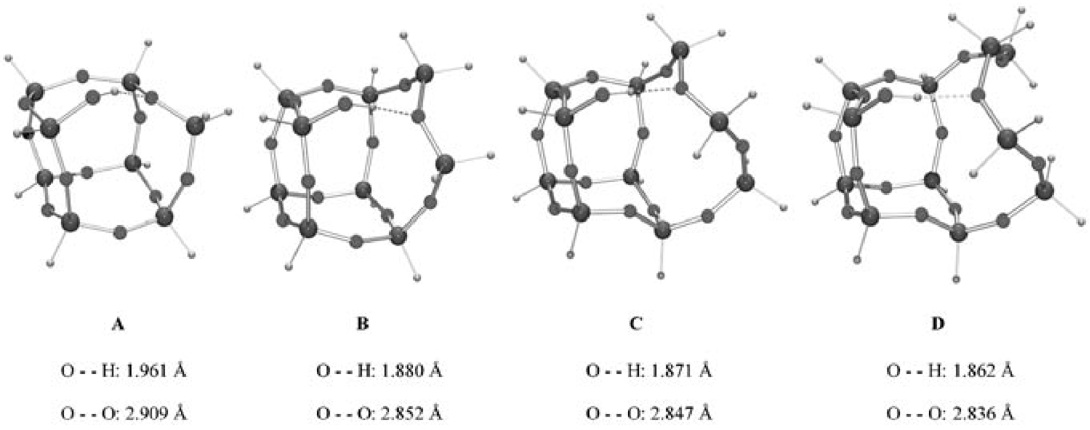

Figure 1. Calculated structures of $H_7Si_7(O\{SiH_2O\}_n)OH$ (n = 1–4).

ed acidity between silanol types are significant and can alter the local reactivity considerably.[7] Acidities are strongly solvent dependent, as the dissociation constant of an acid depends on the ability of the solvent to solvate the proton, the anion, and the undissociated acid. Silsesquioxanes **1**–**7** are highly lypophilic and only dissolve in organic solvents with relatively low polarity like THF or hexane. In solvents with a relatively low dielectric constant such as THF ($\varepsilon_{(20^\circ C)}$ = 7.6), ion pair dissociation hardly occurs.[13] Hence, acidity measurements in low-polar solvents only give qualitative information about relative acidities in each specific solvent; that is, one can only determine whether one compound is more or less acidic than another in a specific solvent. However, this qualitative information is still very significant for ion-exchange reactions and thus for the synthesis of supported catalysts.

The relative Brønsted acidities of the silanols of **1**–**7**, obtained by using the overlapping indicator method to determine the ion-pair acidities (pK_{ip}) in THF from UV/Vis spectra,[13] are given in Table 2. Not surprisingly, owing to intramolecular hydrogen bonding, the relative ion-pair acidities of **1**–**6** are lower than the unperturbed silanols of [(*c*-$C_5H_9)_7Si_8O_{12}(OH)$] and [(*c*-$C_6H_{11})_7Si_8O_{12}(OH)$] (Table 2). Again, compound **1**, with only one -$OSiMe_2O$- unit and thus ample intramolecular hydrogen bonding opportunity, is more acidic than silsesquioxanes **2**–**6**, which contain flexible siloxane rings and stronger hydrogen bonding. Interestingly, there seems to be an optimum in the hydrogen bridging ability of the siloxane ring for **2** and **5**. The larger rings in **3** and **6** probably introduce more steric hindrance, which reduces the effectiveness of the hydrogen bonding as it was not observed in the sterically unhindered model systems [$H_7Si_7(O\{SiH_2O\}_n)OH$] (n = 1–4).

A common method to determine the Brønsted acidity of silica surface silanols consists of monitoring the $\Delta\tilde{\nu}_{OH}$ changes in the IR spectra upon addition of an external proton acceptor (the so-called Badger–Bauer relationship).[13] In the presence of a proton acceptor such as diethyl ether, the $\tilde{\nu}_{OH}$ vibrations shift to lower frequency owing to hydrogen bonding between the silanol and the electron-donating ether. These $\Delta\tilde{\nu}_{OH}$ values can be used as a probe for the energy of the specific interaction and hence the Brønsted acidity of the silanols. Silsesquioxanes **1**–**7** were dissolved in CCl_4 (0.1 M), in the presence of diethyl ether (25 vol %) as the proton acceptor, the $\tilde{\nu}_{OH}$ vibrations shift towards lower wave numbers because of a hydrogen-bonding interaction between the silanol and the external proton acceptor. When the isolated silanol is almost unperturbed (i.e., compound **7** and [(*c*-$C_5H_9)_7Si_8O_{12}(OH)$]), the effect of adding a proton acceptor is largest (a $\Delta\tilde{\nu}_{OH}$ shift of 251 and 359 cm^{-1}, respectively). Compound **1** has, because of its small and rigid siloxane ring, the least possible intramolecular hydrogen bonding compared with compounds **2**–**6**, and undergoes the largest shift under the influence of the added proton acceptor ($\Delta\tilde{\nu}_{OH}$ = 132 cm^{-1}). This is in agreement with the less effective hydrogen bonding in **A** (Figure 1), the calculated structural analogue of **1**. The $\Delta\tilde{\nu}_{OH}$ of at most 132 cm^{-1} for **2**–**6** is considerably smaller than the $\Delta\tilde{\nu}_{OH}$ shift observed when diethyl ether was added to CCl_4 solutions of unperturbed, isolated silanols (Table 2).[7e] Interestingly, when going from a ring-size of six silicon atoms to seven silicon atoms (i.e., from compound **2** to **3** and from compound **5** to **6**) the $\Delta\tilde{\nu}_{OH}$ shift increases by about 60 cm^{-1}, indicating more efficient hydrogen bonding with the external proton donor. This agrees with the observed pK_{ip} values and suggests that the intramolecular siloxane rings in **2** and **5** are more effective donors that the larger siloxy rings in **3** and **6**. The cyclohexyl-substituted compound **4** has a Brønsted acidity similar to that of compound **5** and is even less effected by addition of an external proton donor (for **4** $\Delta\tilde{\nu}_{OH}$ = 16 cm^{-1}, for **5** $\Delta\tilde{\nu}_{OH}$ = 40 cm^{-1}). Apparently, compounds **2** and **5**, with a siloxane ring containing three -$OSiMe_2O$- units, and compound **4**, with a siloxane ring of two -$OSiMe_2O$- units, possess an optimal ring-size; they have the most effective intramolecular hydrogen bonding and thus lowest possible Brønsted acidity. Steric hindrance in **3** and **6** probably prevents effective hydrogen bonding, as no electronic reasons were found for such a large difference in the calculated structures **B**–**D** (Figure 1). Based on the Badger–Bauer relationship, compound **7** seems more acidic than **2**–**6**. However, the pK_{ip} (11.1) of **7** suggests an acidity similar to that of **2**–**6**, and considerably lower than that of the truly isolated silanols [(*c*-$C_5H_9)_7Si_8O_{12}(OH)$] (pK_{ip} 8.9) and [(*c*-$C_6H_{11})_7Si_8O_{12}(OH)$] (p$K_{ip}$ 9.0). Possibly, deprotonation of the silanol by the sterically hindered fluorenyl indicators is hampered by the bulky phenyl substituents.

Substitution reactions with $GaMe_3$: Owing to their Lewis acidic character, gallium siloxides and alkoxides generally form aggregated structures or Lewis base adducts with tetrahedrally surrounded gallium centers.[14,15] With **1**–**7** available, we were interested to see whether the intramolecular electron donation of the neighboring siloxide oxygens can effectively coordinate to the Lewis acidic gallium center, suppressing the commonly observed tendency to reduce the metal's electron deficiency by forming aggregates. When reacting **1**, **6**, and **7** with an equimolar amount of $GaMe_3$, gallium species [(*c*-$C_5H_9)_7Si_7O_{10}(OSiMe_2O)(GaMe_2)]_2$ **8**, [(*c*-$C_6H_{11})_7Si_7O_{10}(O\{SiMe_2O\}_4)(GaMe_2)]_2$ **9**, and [(*c*-$C_5H_9)_7Si_7O_{10}(OSiPh_2O)(GaMe_2)]_2$ **10** could be isolated as crystalline materials (Scheme 2). Unfortunately, only **10** gave crystals suitable for an X-ray structure analysis (Figure 2). Molecular weight determination in solution, performed using melting point depression studies in benzene, demonstrated that all gallium species are dimeric in solution. Hence, the electron donating ability of the siloxide functionalities in **1**, **6**, and **7** is not sufficient to satisfy the electron deficiency of the gallium silsesquioxanes **8**–**10**, which form dimeric structures with bridging siloxide units rather than Lewis base adducts with coordinated siloxide functionalities.

The structure of **10** clearly shows that the sterically demanding $Ph_2Si(O\text{-})_2$ fragment does not allow much electron donation by the siloxane oxygens. Most probably, the same is true in the case of silanol **7**, which explains the absence of intramolecular hydrogen bonding in **7**. The Ga–O bond length in **10** (1.97(7) Å) is comparable to those observed for {[(*c*-$C_5H_9)_7Si_7O_{12})]_2(GaMe_2)_6$} (1.99(3) Å) and {[(*c*-

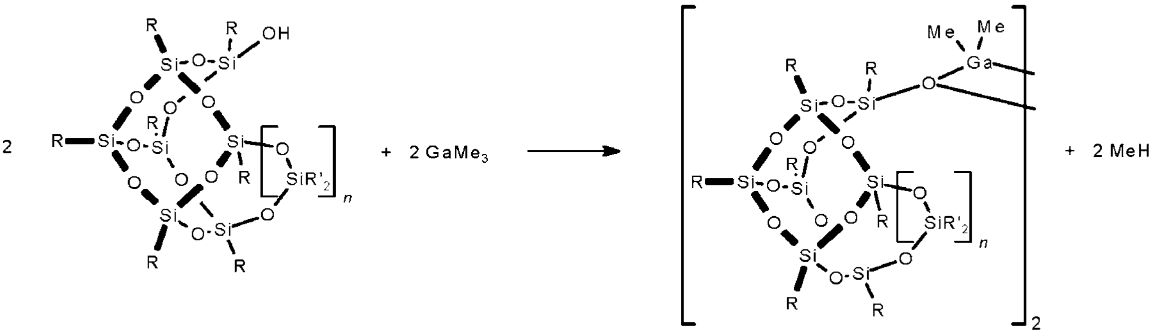

Scheme 2. Synthesis of dimethyl gallium silsesquioxanes **8**–**10**.

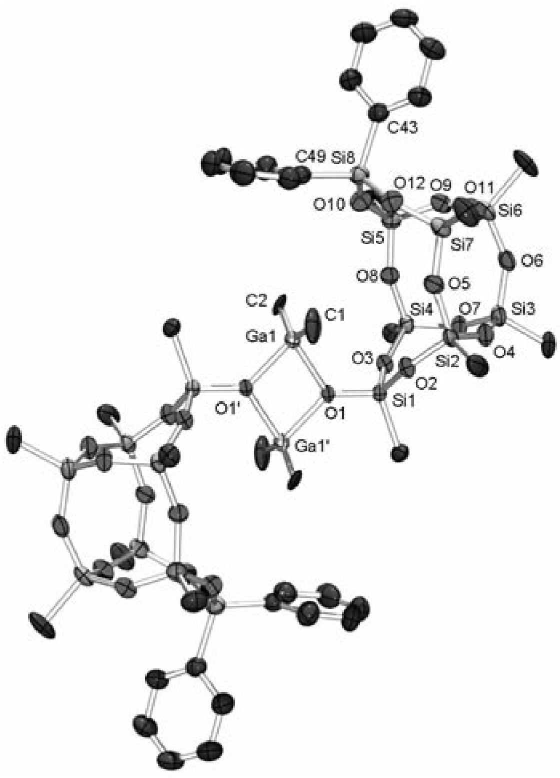

Figure 2. Molecular structure of $[(c\text{-}C_5H_9)_7Si_7O_{10}(OSiPh_2O)(GaMe_2)]_2$ **10**. Thermal ellipsoids are scaled to enclose 40% of the electron density. Only the methyne carbons of the cyclopentyl rings are shown for clarity. Selected bond lengths [Å]: Ga1−C1, 2.026(1); Ga1−C2, 1.961(1); Ga1−O1, 1.989(1); Ga1−O1′, 1.973(1); Ga1−Ga1′, 2.995(1); Si1−O1, 1.617(3); Si1−O2, 1.615(4); Si1−O3, 1.636(4); Si2−O2, 1.628(4); Si2−O4, 1.621(4); Si2−O5, 1.624(4); Si3−O4, 1.628(4); Si3−O6, 1.634(4); Si6−O6, 1.622(4); Si6−O11, 1.634; Si7−O5, 1.622(4); Si7−O11, 1.624(4); Si7−O12, 1.631(4); Si8−O10, 1.642(4); Si8−O12, 1.629(4); Si8−C43, 1.865(6); Si8−C49, 1.845(7). Selected angles [°]: C1-Ga1-C2, 128.2(1); C1-Ga1-O1, 112.1(1); C2-Ga1-O1, 106.2(4); O1-Ga1-O1′, 81.7(7); Ga1-O1-Ga1′, 58.0(8); O1-Si1-O2, 108.2(7); O1-Si1-O3, 107.9(4); O2-Si1-O3, 110.0(0); O2-Si2-O4, 108.9(2); Si2-O4-Si3, 142.25(3); O4-Si3-O6, 109.75(3); Si3-O6-Si6, 145.55(3); O6-Si6-O11, 109.78(3); Si6-O11-Si7, 144.98(3); O11-Si7-O12, 108.96(3); Si7-O12-Si8, 145.7(3); O10-Si8-O12, 111.2(3); O10-Si8-C43, 107.7(3); O10-Si8-C49, 109.9(3); O12-Si8-C43, 110.4(3); O12-Si8-C49, 108.5(3); C43-Si8-C49, 109.1(3).

$C_5H_9)_7Si_7O_{11}(OSiMePh_2)]_2(GaMe_2)_4\}$ (1.97(4) Å), which were obtained by reacting $GaMe_3$ with $(c\text{-}C_5H_9)_7Si_7O_9(OH)_3$ and $(c\text{-}C_5H_9)_7Si_7O_9(OH)_2OSiMePh_2$, respectively.[14e] Also the Si1−O1 distances (1.617(3) Å) in **10** are very similar to the Si−O distances of other reported silsesquioxane–gallium species such as $\{[(c\text{-}C_5H_9)_7Si_7O_{11}(OSiMePh_2)]_2(GaMe_2)_4\}$ ((1.622(2) Å) and $\{[(c\text{-}C_5H_9)_7Si_7O_{12})]_2(GaMe_2)_6\}$ (1.618(3) Å).[14e] The $[\mu(\equiv SiO)GaMe_2]_2$ fragment in **10** is unperturbed and shows no indication of interacting with the $Ph_2Si(O\text{-})_2$ fragments.[14] ^1H and ^{13}C NMR spectra of **10** show one gallium–methyl peak situated at normal high-field resonances (^1H: δ = 0.28; ^{13}C: δ = −2.85), indicating that the methyl groups are equivalent in solution.

Substitution reactions with $[Cp''Ti(CH_2Ph)_3]$ (Cp'' = η^5-1,3-$C_5H_3(SiMe_3)_2$): The active species of Group 4 metal olefin polymerization catalysts are highly Lewis acidic and are known to interact with various substrates like aromatics and even generally inert C−H and C−F bonds, to reduce their electron deficiency.[18a] With **1**–**7** available, we were interested in the coordinating ability of the adjacent siloxide functionalities to cationic titanium centers and the consequent effect on the catalyst's stability and activity. As characteristic examples, **1** and **4** were reacted with a stoichiometric amount of $[Cp''Ti(CH_2Ph)_3]$. The gradual formation of the corresponding titanium half-sandwich products $Cp''[(c\text{-}C_5H_9)_7Si_7O_{10}(OSiMe_2O)]Ti(CH_2Ph)_2$ **11** and $Cp''[(c\text{-}C_6H_{11})_7Si_7O_{10}(O\{SiMe_2O\}_2)]Ti(CH_2Ph)_2$ **12** was followed by room-temperature ^1H NMR. The methylene protons of the benzyl groups in **11** and **12** are diastereotopic, which results in a characteristic AB spin system. The ^1H and ^{13}C NMR resonances of the benzyl methylene group of **11** (^1H: δ = 3.30, 2.46, $^3J_{H\text{-}H}$ = 9.9 Hz; ^{13}C: δ = 85.42, $^1J_{C\text{-}H}$ = 125 Hz) and **12** (^1H: δ = 3.46, 2.39, $^3J_{H\text{-}H}$ = 9.9; ^{13}C: δ = 85.76, $^1J_{C\text{-}H}$ = 125 Hz) show similar chemical shifts as in the earlier reported $Cp''[(c\text{-}C_5H_9)_7Si_8O_{13}]Ti(CH_2Ph)_2$ (^1H: δ = 3.45, 2.12, $^3J_{H\text{-}H}$ = 9.6 Hz; ^{13}C: δ = 86.83, $^1J_{C\text{-}H}$ = 127 Hz).[16] As was also observed for $(c\text{-}C_5H_9)_7Si_8O_{12}(OH)$, $[Cp''Ti(CH_2Ph)_3]$ reacts exclusively with one equivalent of the silsesquioxanes **1** and **4**. Attempts to force **11** and **12** to react with a second equivalent of the silsesquioxanes **1** or **4**, respectively, failed. Complexes **11** and **12** were isolated as viscous oils after evaporation of the hydrocarbon solvent. Attempts to purify them by crystallization failed. Therefore, for further studies the complexes were prepared in situ in $[D_6]$benzene and used without further purification.

1-Hexene polymerization of 11, 12, $[Cp''[(c\text{-}C_5H_9)_7Si_8O_{13}]Ti(CH_2Ph)_2]$, and $[Cp''Ti(CH_2Ph)_3]$: Polymerization of 1-

hexene with the described titanasilsesquioxane benzyl complexes were performed using $B(C_6F_5)_3$ and $[Ph_3C]^+[B(C_6F_5)_4]^-$ as cocatalysts. Although alkyl abstraction by $B(C_6F_5)_3$ is an equilibrium reaction, generally, the reaction of Group 4 metal alkyls with $B(C_6F_5)_3$ results in quantitative formation of the cationic Group 4 metal species and the corresponding borate.[17,18] For Cp″[(*c*-$C_5H_9)_7Si_8O_{13}$]Ti($CH_2Ph)_2$, **11**, and **12** the equilibrium constant of the benzyl abstraction reaction is considerably lower (K≈0.3) and even with four equivalents of $B(C_6F_5)_3$, the catalyst activity is an order of magnitude lower than when $[Ph_3C]^+[B(C_6F_5)_4]^-$ is used as cocatalyst (Table 3). To study the effect of siloxane functionalities in the proximity of the active site on the catalyst's performance and stability, isoperibolic polymerizations with $[Ph_3C]^+[B(C_6F_5)_4]^-$ as cocatalyst were followed in time. The heat development versus time plot (Figure 3) thus obtained gives a qualitative measure for the polymerization rate.

Table 3. 1-Hexene polymerization results for **11**, **12**, Cp″[(*c*-$C_5H_9)_7Si_8O_{13}$]Ti($CH_2Ph)_2$, and [Cp″Ti($CH_2Ph)_3$].

Catalytic system	Yield [g]	Conversion [%]	M_n [g mol^{-1}]	M_w [g mol^{-1}]	M_w/M_n
11 + $B(C_6F_5)_3$ [a]	1.39	(21)	5912	13857	2.3
11 + $[Ph_3C]^+[B(C_6F_5)_4]^-$[b]	6.07	(91)	3483	8240	2.4
12 + $B(C_6F_5)_3$[a]	0.64	(10)	4428	10431	3.1
12 + $[Ph_3C]^+[B(C_6F_5)_4]^-$[b]	6.10	(91)	2922	6804	2.3
Cp″[(*c*-$C_5H_9)_7Si_8O_{13}$]Ti($CH_2Ph)_2$ + $B(C_6F_5)_3$[a]	0.53	(8)	2820	9838	3.5
Cp″[(*c*-$C_5H_9)_7Si_8O_{13}$]Ti($CH_2Ph)_2$ + $[Ph_3C]^+[B(C_6F_5)_4]^-$[b]	5.69	(85)	2380	6310	2.7
Cp″Ti($CH_2Ph)_3$ + $[Ph_3C]^+[B(C_6F_5)_4]^-$[b]	4.53	(68)	5848	15931	2.7

[a] 10 μmol catalyst, 40 μmol cocatalyst, reaction stopped after 24 h. [b] 10 μmol catalyst, 11 μmol cocatalyst, reaction followed in time over 6 h

The yield of atactic poly-1-hexene (over 90 % in all cases) suggests that the maximum in the temperature curve is reached when almost all 1-hexene is consumed and the temperature decreases thereafter as a result of starvation. The catalytic performance of the titanasilsesquioxanes is comparable to that of other half-sandwich complexes. As can clearly be seen from Figure 3, there is a noticeable effect of the siloxy ring in **11** and **12**. Whereas the activity for Cp″[(*c*-$C_5H_9)_7Si_8O_{13}$]Ti($CH_2Ph)_2$ and [Cp″Ti($CH_2Ph)_3$] rapidly reaches its optimum, for both **11** and **12**, activation seems surprisingly slow, taking up to two hours to reach maximum heat formation. For **11** it seems to be an initiation problem; for **12** the retarding effect is more persistent, as the heat produced is considerably less than for **11**. Generally, catalyst activation by $[Ph_3C]^+[B(C_6F_5)_4]^-$ is instantaneous, which makes it unlikely that the retarding effect is caused by slow initiation.[18] To verify this, activation of **11**, **12**, and Cp″[(*c*-$C_5H_9)_7Si_8O_{13}$]Ti($CH_2Ph)_2$ with $[Ph_3C]^+[B(C_6F_5)_4]^-$ was subjected to a spectroscopic investigation. In all cases, the ^1H NMR spectra ([D$_5$]bromobenzene, 25 °C) showed immediate formation of $C_6H_5CH_2CPh_3$ (δ = 3.82) and disappearance of the AB pattern from the diastereotopic CH_2 of the starting compounds. Over time, no significant changes that might indicate degeneration of the ionic species were found in ^1H or ^{19}F NMR spectra. Hence, formation of the cation is instantaneous in all cases, but the siloxane rings seem to hamper (initial) polymerization in some way. Based on the earlier observed tendency of **4**, and to a lesser extend **1**, to form intramolecular hydrogen bonds between the siloxy ring and the silanol, it is very well possible that the siloxane rings in **12** and **11** (but to a lesser extent) act as a Lewis base for the cationic titanium center, thus lowering the catalytic activity. The steric strain of the growing chain might reduce the coordination ability of the siloxane ring, especially when this is already weak as in **11**. This could explain why **11** shows an activity similar to Cp″[(*c*-$C_5H_9)_7Si_8O_{13}$]Ti($CH_2Ph)_2$ and Cp″Ti($CH_2Ph)_3$, while the activity of **12** seems to lag behind. The optimized (DFT calculations, B3LYP) molecular structures of $[H_7Si_7(O\{SiH_2O\}_n)O\text{-}Ti(C_5H_5)CH_3]^+$ (n = 1, 2), showed the expected interaction of the adjacent silylether function with the cationic metal center. As expected, the interaction between the titanium and the neighboring silylether is slightly weaker in the model for **11** (2.137 Å) than in the stripped version of **12** (2.127 Å).

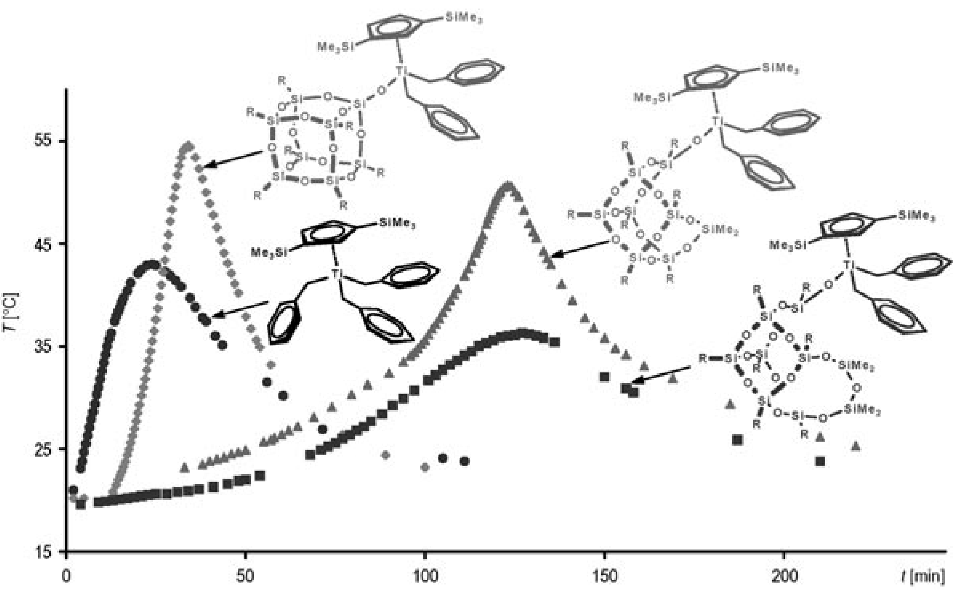

Figure 3. Isoperibolic 1-hexene polymerization of **11**, **12**, Cp″[(*c*-$C_5H_9)_7$-Si_8O_{13}]Ti($CH_2Ph)_2$, and [Cp″Ti($CH_2Ph)_3$] activated with $[Ph_3C]^+[B(C_6F_5)_4]^-$.

Once it was clear that the siloxane rings definitely have an effect on the catalytic activity of these systems, we also studied whether the siloxide functionalities affect the stability of the systems. For this study, complexes **11**, **12**, and Cp″[(*c*-$C_5H_9)_7Si_8O_{13}$]Ti($CH_2Ph)_2$ were treated with one equivalent of B($C_6F_5)_3$ in [D_8]toluene and the formation of the cationic species was followed over time at 25 °C by ^{19}F NMR spectroscopy (Figure 4). In all cases only part of the B($C_6F_5)_3$ is consumed owing to an equilibrium between titanium dialkyl + borane and the cation + borate (Scheme 3). Whereas the maximum conversion for Cp″[(*c*-$C_5H_9)_7Si_8O_{13}$]Ti($CH_2Ph)_2$ and **11** is about 30 %, for **12** it is only 15 %. The reason for this difference can either be steric or electronic. The larger siloxane ring in **12** induces more steric hindrance in the proximity of the titanium center, which might hamper the ability of the B($C_6F_5)_3$ to get close enough to the titanium to abstract a benzyl group. Alternatively, the oxygen atoms of the siloxane ring can also coordinate to the Lewis acidic B($C_6F_5)_3$, preventing it from abstracting the benzyl group. However, this should be visible in the ^{19}F NMR spectrum, which is not the case. Aside from unreacted B($C_6F_5)_3$, the ^{19}F NMR spectra for all three complexes revealed the presence of two types of borates. The difference in chemical shift between the F_{meta} and F_{para} resonances (Table 4) suggests the presence of both solvent-separated ion pairs and contact ion pairs.[17,19] In addition, a second borane $PhCH_2B(C_6F_5)_2$ is present in low concentration. This is formed as the result of exchange of a boron pentafluorophenyl substituent with a titanium benzyl group, and has been observed for several metal alkyl systems.[18,20] For both **11** and **12**, the amount of $PhCH_2B(C_6F_5)_2$ remains very low throughout the experiment (1000 min). On the other hand, for the Cp″[(*c*-$C_5H_9)_7Si_8O_{13}$]Ti($CH_2Ph)_2$/B($C_6F_5)_3$ system the amount of $PhCH_2B(C_6F_5)_2$ gradually increases, which suggests a lower stability of the system when adjacent siloxide functionalities are absent.

Conclusion

Silica surface silanols in the proximity of siloxide functionalities have been mimicked using silsesquioxanes of the type $R_7Si_7O_9(O\{SiR'_2O\}_{n+1})(OH)$ (R = *c*-C_5H_9, *c*-C_6H_{11}; R′ = Me, Ph; n = 0–3). NMR and FTIR studies show that the neighboring siloxane ring lowers the acidity of the silanol considerably as a result of effective intramolecular hydrogen bonding between the two. The most effective intramolecular hydrogen bonding and thus lowest possible Brønsted acidity was found for compounds **2**, **4**, and **5** and is dependent on the siloxane ring size. However, the electron-donating ability of the siloxide functionalities in **1**, **6**, and **7** proved not to be sufficient to satisfy the electron deficiency of the gallium silsesquioxanes **8**–**10**, which form dimeric structures with bridging siloxide units rather than Lewis base adducts with coordinated siloxide functionalities. Cationic titanium half-sandwich complexes provided soluble models for silica-grafted olefin polymerization catalysts that can undergo interactions with neighboring siloxane functionalities. It was found that competitive coordination of the siloxide oxygens to the cationic site retards the polymerization. Whereas a gradual decomposition and formation of $PhCH_2B(C_6F_5)_2$ was observed for the Cp″[(*c*-$C_5H_9)_7Si_8O_{13}$]Ti($CH_2Ph)_2$/B($C_6F_5)_3$ system, the cationic titanium species formed by reacting **11** and **12** with B($C_6F_5)_3$ are stable for a long period of time. This clearly demonstrates the positive effect of siloxide coordination on the stability of the cationic species.

Experimental Section

General: When necessary, reactions were performed under an argon atmosphere using a glove box (Braun MB-150 GI) and Schlenk techniques. Solvents were distilled from K (methylcyclohexane, THF), Na (toluene), Na/K alloy (hexanes, [D_6]benzene), and Na/benzophenone (Et_2O); or dried over 4 Å molecular sieves (NEt_3, CCl_4, $CDCl_3$, [D_8]toluene, [D_5]bromobenzene) and stored under argon. ^{1}H and ^{13}C NMR spectra were recorded on a Varian Mercury 400 spectrometer (25 °C, ^{1}H NMR: 400 MHz, ^{13}C NMR: 100.6 MHz). ^{29}Si NMR spectra were recorded on a

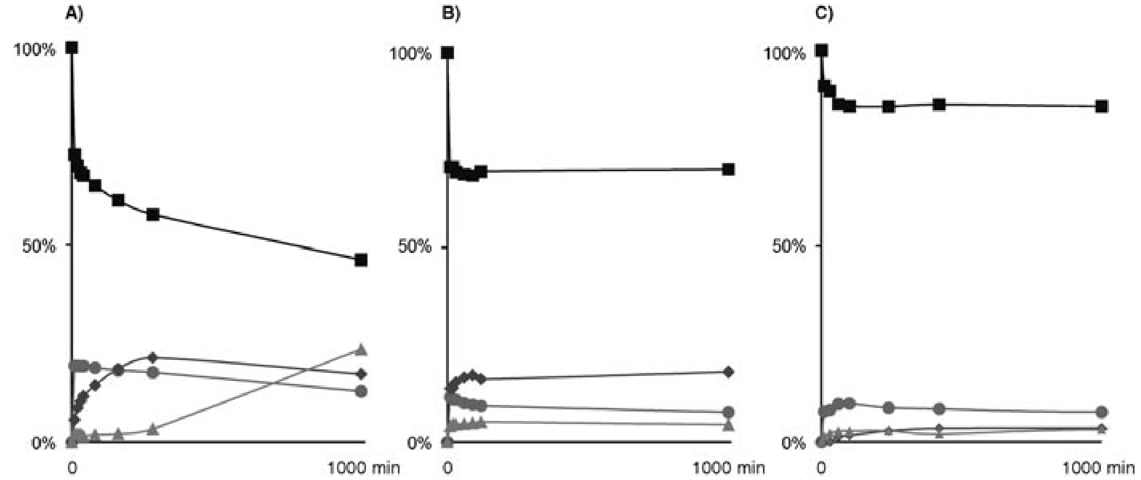

Figure 4. Conversion of B($C_6F_5)_3$ (■) with **A**: Cp″[(*c*-$C_5H_9)_7Si_{12}O_{13}$]Ti($CH_2Ph)_2$, **B**: **11**, and **C**: **12** into solvent-separated ion pairs (◆), contact ion pairs (●), and in the neutral $C_6H_5CH_2B(C_6F_5)_2$ (▲).

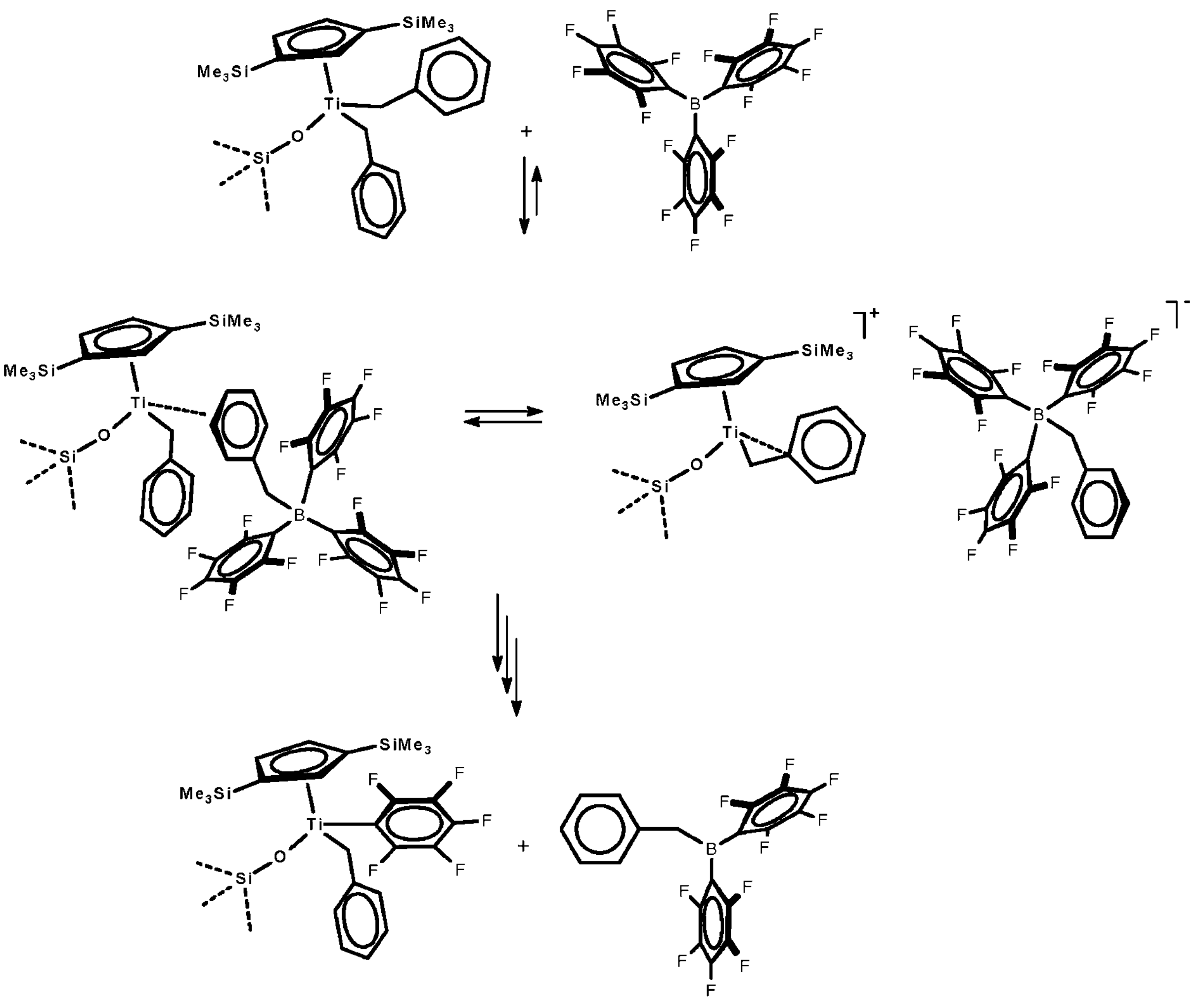

Scheme 3. Formation of solvent-separated and contact ion pairs of titanasilsesquioxanes with $B(C_6F_5)_3$ and disproportionation.

Table 4. ^{19}F NMR data of the ion pairs of **11**, **12**, and $Cp''[(c\text{-}C_5H_9)_7Si_8O_{13}]Ti(CH_2Ph)_2$ with $B(C_6F_5)_3$.

Complex	Ion pair	δ $^{19}F_{ortho}$[a]	δ $^{19}F_{para}$[a]	δ $^{19}F_{meta}$[a]	$\Delta\delta(F_m-F_p)$[a]
11	$\{Cp''[(c\text{-}C_5H_9)_7Si_8O_{10}(O_2SiMe_2)]\text{-}TiCH_2Ph\}^+$ $\{PhCH_2B(C_6F_5)_3\}^-$; solvent separated ion pair	−129.53	−163.94	−166.58	2.64
11	$\{Cp''[(c\text{-}C_5H_9)_7Si_8O_{10}(O_2SiMe_2)]\text{-}TiCH_2Ph\}^+$ $\{PhCH_2B(C_6F_5)_3\}^-$; contact ion pair	−129.53	−160.30	−164.45	4.15
12	$\{Cp''[(c\text{-}C_5H_9)_7Si_8O_{10}([OSiMe_2]_2O)]\text{-}TiCH_2Ph\}^+$ $\{PhCH_2B(C_6F_5)_3\}^-$; solvent separated ion pair	−129.65	−163.95	−166.52	2.57
12	$\{Cp''[(c\text{-}C_5H_9)_7Si_8O_{10}([OSiMe_2]_2O)]\text{-}TiCH_2Ph\}^+$ $\{PhCH_2B(C_6F_5)_3\}^-$; contact ion pair	−129.65	−160.11	−164.29	4.18
$Cp''[(c\text{-}C_5H_9)_7Si_8O_{13}]\text{-}Ti(CH_2Ph)_2$	$\{Cp''[(c\text{-}C_5H_9)_7Si_8O_{13}]TiCH_2Ph\}^+$ $\{PhCH_2B(C_6F_5)_3\}^-$; solvent separated ion pair	−129.71	−163.70	−166.49	2.79
$Cp''[(c\text{-}C_5H_9)_7Si_8O_{13}]\text{-}Ti(CH_2Ph)_2$	$\{Cp''[(c\text{-}C_5H_9)_7Si_8O_{13}]TiCH_2Ph\}^+$ $\{PhCH_2B(C_6F_5)_3\}^-$; contact ion pair	−129.71	−160.34	−164.45	4.11

[a] ^{19}F NMR spectra (471 MHz, 25 °C, $[D_8]$toluene) are referenced using an external standard CF_3CO_2H at $\delta = -76.3$.

Varian Indigo 500 spectrometer (25 °C, ^{19}F NMR: 471.0 MHz; ^{29}Si NMR: 99.3 MHz). Chemical shifts are reported in ppm and referenced to residual solvent resonances (^1H, ^{13}C NMR) or an external standard (^{19}F NMR: CF_3CO_2H in $CDCl_3$ $\delta = -76.3$; ^{29}Si: $SiMe_4$ $\delta = 0$ ppm). IR spectra were recorded at room temperature on a Nicolet Avatar 360 FTIR spectrophotometer. Samples in solution were prepared under inert atmosphere (glove box), $\tilde{\nu}_{OH}$ values were determined in 0.1 M CCl_4 solutions and $\Delta\tilde{\nu}_{OH}$ in 0.1 M CCl_4 solutions containing 0.25 M diethyl ether. Solid-state samples were recorded as Nujol mulls (prepared under nitrogen, glove box). UV measurements for determination of the pK_{ip} values, were performed on a UV-2401PC spectrophotometer with standard slide width and scan speed. The determination of pK_{ip} values was performed as reported elsewhere.[7g,h] Elemental analyses were carried out at the Analytical Department of the University of Groningen (compounds **8**–**10**) and at the Analytical Department of the Technical University of Eindhoven (compounds **1**–**7**); quoted data are the average of at least two independent measurements. The molecular weights, number-average molecular weights, and molecular weight distributions were determined by gel permeation chromatography (GPC) using THF as solvent and standard parameters, at the Department of Polymer Chemistry, Eindhoven. Starting materials $R_7Si_7O_9(OH)_3$ (R = *c*-C_5H_9, *c*-C_6H_{11}), (*c*-C_5H_9)$_7$$Si_7O_9(OH)_2O$-$SiMe_3$ and (*c*-C_5H_9)$_7$$Si_8O_{12}(OH)$,[7] Cp″Ti($CH_2Ph$)$_3$[21] and $B(C_6F_5)_3$,[22] and $[Ph_3C]^+[B(C_6F_5)_4]^-$[23] were prepared following literature procedures.

(*c*-C_5H_9)$_7$$Si_7O_9(OSiMe_2O)OH$ (1): Cl_2SiMe_2 (1.05 g, 8.14 mmol, 0.95 equiv) was slowly added to a solution of (*c*-C_5H_9)$_7$$Si_7O_9(OH)_3$ (7.50 g, 8.56 mmol) and NEt_3 (2.4 mL, 17.3 mmol) in THF (150 mL). The mixture was stirred overnight at room temperature and then filtered in order to remove most of the $Et_3N(H)Cl$. After evaporation of THF, hexanes (100 mL) was added, and the mixture was heated to dissolve the product completely. Upon cooling in air, the last traces of $Et_3N(H)Cl$ precipitated from the mixture as flakes and could be filtered easily. Thorough drying yielded product **1** as a white (slightly hygroscopic) powder (6.70 g, 7.19 mmol, 84%). M.p. 174°C; ^{1}H NMR ([D]chloroform): δ = 3.16 (s, 1H; SiO*H*), 1.79 (m, 14H; C*H*$_2$-C_5H_9), 1.62 (m, 14H; C*H*$_2$-C_5H_9), 1.53 (m, 28H; C*H*$_2$-C_5H_9), 1.02 (m, 7H; C*H*-C_5H_9), 0.23 (s, 3H; O(SiC*H*$_3$)$_2$O), 0.21 (s, 3H; O(SiC*H*$_3$)$_2$O); ^{13}C NMR ([D]chloroform): δ = 27.38, 27.28, 27.07, 26.99 (*C*H$_2$-C_5H_9), 22.90, 22.60, 22.34, 22.26, 22.19 (2:2:1:1:1 ratio; *C*H-C_5H_9), 0.73, 0.04 (1:1 ratio; OSi(*C*H$_3$)$_2$O); ^{29}Si NMR ([D]chloroform): δ = −16.02 (O*Si*(CH$_3$)$_2$O), −56.04 (*Si*-OH), −65.29, −65.33, −65.79, −67.30 (1:1:2:2 ratio; O$_3$*Si*C_5H_9); IR: $\tilde{\nu}$ = 3557 (w), 2947 (s), 2864 (s), 1450 (w), 1257 (w), 1079 (vs), 911 (w), 875 (w), 844 (w), 802 (w), 774 (w), 722 cm^{-1} (w); elemental analysis calcd for $C_{37}H_{70}O_{12}Si_8$ (931.64): C 47.70, H 7.57; found C 47.84, H 7.41.

(*c*-C_5H_9)$_7$$Si_7O_9(O\{SiMe_2O\}_3)OH$ (2): A similar procedure as for compound **1** afforded **2** as a white powder (82%). M.p. 168°C; ^{1}H NMR ([D]chloroform): δ = 3.91 (s, 1H; SiO*H*), 1.78 (m, 14H; C*H*$_2$-C_5H_9), 1.63 (m, 14H; C*H*$_2$-C_5H_9), 1.52 (m, 28H; C*H*$_2$-C_5H_9), 0.98 (m, 7H; C*H*-C_5H_9), 0.23 (s, 3H; O{Si(C*H*$_3$)$_2$O}$_3$), 0.19 (s, 6H; O{Si(C*H*$_3$)$_2$O}$_3$), 0.18 (s, 6H; O{Si(C*H*$_3$)$_2$O}$_3$), 0.14 (s, 3H; O{Si(C*H*$_3$)$_2$O}$_3$); ^{13}C NMR ([D]chloroform): δ = 27.45, 27.27, 27.13, 27.01 (*C*H$_2$-C_5H_9), 23.67, 23.11, 22.96, 22.79, 22.26 (2:1:2:1:1 ratio; *C*H-C_5H_9), 0.91, 0.82, 0.70, 0.52 (1:2:2:1 ratio; O{Si(*C*H$_3$)$_2$O}$_3$); ^{29}Si NMR ([D]chloroform): δ = −17.68, −19.74 (O{*Si*(CH$_3$)$_2$O}$_3$, 1:2), −59.27 (*Si*OH), −65.54, −67.47, −68.21, −69.18 (1:2:1:2 ratio; O$_3$*Si*C_5H_9); IR: $\tilde{\nu}$ = 3528 (w), 2948 (s), 2864 (s), 1451 (w), 1259 (m), 1070 (vs), 948 (w), 910 (w), 844 (w), 802 (m), 715 cm^{-1}(w); elemental analysis calcd for $C_{41}H_{82}O_{14}Si_{10}$ (1079.95): C 45.60, H 7.65; found C 45.40, H 7.68.

(*c*-C_5H_9)$_7$$Si_7O_9(O\{SiMe_2O\}_4)OH$ (3): A similar procedure was used as for **1**. Reaction at 40°C overnight yielded **3** as a white wax (81%). Owing to its high solubility in organic solvents, the compound could not be purified. A sample suitable for elemental analysis was not obtained. M.p. 149–52°C; ^{1}H NMR ([D]chloroform): δ = 3.64 (s, 1H; SiO*H*), 1.78 (m, 14H; C*H*$_2$-C_5H_9), 1.62 (m, 14H; C*H*$_2$-C_5H_9), 1.51 (m, 28H; C*H*$_2$-C_5H_9), 0.98 (m, 7H; C*H*-C_5H_9), 0.19 (s, 6H; O{Si(C*H*$_3$)$_2$O}$_4$), 0.17 (s, 12H; O{Si(C*H*$_3$)$_2$O}$_4$), 0.14 (s, 6H; O{Si(C*H*$_3$)$_2$O}$_4$); ^{13}C NMR ([D]chloroform): δ = 27.55, 27.30, 27.02 (*C*H$_2$-C_5H_9), 24.04, 23.51, 23.05, 22.99, 22.38 (2:1:2:1:1 ratio; *C*H-C_5H_9), 1.09, 0.98, 0.83 (2:4:2 ratio; O{Si(*C*H$_3$)$_2$O}$_4$); ^{29}Si NMR ([D]chloroform): δ = −20.27, −21.07 (2:2 ratio; O{*Si*Me$_2$}$_4$O)), −58.95 (*Si*-OH), −65.62, −67.14, −69.14, −69.18 (1:2:1:2 ratio; O$_3$*Si*C_5H_9); IR: $\tilde{\nu}$ = 3567 (w), 2949 (m), 2865 (m), 1451 (w), 1259 (m), 1067 (s), 948 (w), 910 (w), 844 (w), 800 (m), 714 cm^{-1} (w).

(*c*-C_6H_{11})$_7$$Si_7O_9(O\{SiMe_2O\}_2)OH$ (4): A similar procedure as for compound **1** afforded **4** as a white powder (83%). M.p. 159°C; ^{1}H NMR ([D]chloroform): δ = 3.64 (s, 1H; SiO*H*), 1.77 (m, 35H; C*H*$_2$-C_6H_{11}), 1.26 (m, 35H; C*H*$_2$-C_6H_{11}), 0.78 (m, 7H; C*H*-C_6H_{11}), 0.20 (d, 12H; O{Si(C*H*$_3$)$_2$O}$_2$); ^{13}C NMR ([D]chloroform): δ = 27.59, 26.80, 26.54, (*C*H$_2$-C_6H_{11}), 24.27, 23.81, 23.77, 23.46, 23.07(2:2:1:1:1 ratio; *C*H-C_6H_{11}), 0.93, 0.43 (2:2 ratio; O{Si(*C*H$_3$)$_2$O}$_2$); ^{29}Si NMR ([D]chloroform): δ = −17.92 (O{*Si*(CH$_3$)$_2$O}$_2$), −67.66, −69.72, −70.09, −70.26 (1:2:1:2 ratio; O$_3$*Si*C_5H_9), −60.32 (*Si*OH); IR: $\tilde{\nu}$ = 3588 (w), 2919 (s), 2848 (s), 1447 (w), 1261 (m), 1195 (m), 1067 (s), 893 (m), 846 (m), 803 (m), 751 cm^{-1} (w); elemental analysis calcd for $C_{46}H_{90}O_{13}Si_9$ (1103.99): C 50.05, H 8.22; found C 49.52, H 7.94.

(*c*-C_6H_{11})$_7$$Si_7O_9(O\{SiMe_2O\}_3)OH$ (5): A similar procedure as for compound **1** gave **5** as a white powder (66%). M.p. 142°C; ^{1}H NMR ([D]chloroform): δ = 3.94 (s, 1H; SiO*H*), 1.78 (m, 35H; C*H*$_2$-C_6H_{11}), 1.26 (m, 35H; C*H*$_2$-C_6H_{11}), 0.77 (m, 7H; C*H*-C_6H_{11}), 0.21 (s, 3H; O{Si(C*H*$_3$)$_2$O}$_3$), 0.18 (d, 12H; O{Si(C*H*$_3$)$_2$O}$_3$), 0.13 (s, 3H; O{Si(C*H*$_3$)$_2$O}$_3$); ^{13}C NMR ([D]chloroform): δ = 27.63, 27.51, 26.85, 26.72, (*C*H$_2$-C_6H_{11}), 24.57, 24.17, 23.99, 23.75, 23.06 (2:1:2:1:1 ratio; *C*H-C_6H_{11}), 0.96, 0.85, 0.68, 0.56 (1:2:2:1 ratio; O{Si(*C*H$_3$)$_2$O}$_3$); ^{29}Si NMR ([D]chloroform): δ = −17.50, −19.68 (1:2 ratio; O{Si(C*H*$_3$)$_2$O}$_3$), −61.53 (*Si*-OH), −67.70, −69.68, −70.49, −71.10 1:2:1:2 ratio; O$_3$*Si*C_5H_9); IR: $\tilde{\nu}$ = 3595 (w), 2919 (s), 2848 (s), 1447 (m), 1260 (m), 1196 (m), 1067 (vs), 893 (m), 846 (m), 801 (m), 748 cm^{-1} (w); elemental analysis calcd for $C_{48}H_{96}O_{14}Si_{10}$ (1178.14): C 48.94, H 8.21; found C 48.60, H 8.24.

(*c*-C_6H_{11})$_7$$Si_7O_9(O\{SiMe_2O\}_4)OH$ (6): A similar procedure was used as for compound **1**. Reaction at 40°C overnight, afforded **6** as white powder (60%). M.p. 116°C; ^{1}H NMR ([D]chloroform): δ = 3.47 (s, 1H; SiO*H*), 1.77 (m, 35H; C*H*$_2$-C_6H_{11}), 1.27 (m, 35H; C*H*$_2$-C_6H_{11}), 0.76 (m, 7H; C*H*-C_6H_{11}), 0.18 (s, 6H;O{Si(C*H*$_3$)$_2$O}$_4$), 0.17 (s, 6H; O{Si(C*H*$_3$)$_2$O}$_4$), 0.15 (s, 6H; O{Si(C*H*$_3$)$_2$O}$_4$), 0.13 (s, 6H; O{Si(C*H*$_3$)$_2$O}$_4$); ^{13}C NMR ([D]chloroform): δ = 27.81, 27.67, 27.52, 26.92, 26.84, 26.85 (*C*H$_2$-C_6H_{11}), 24.88, 24.61, 23.99, 23.09 (2:1:3:1 ratio; *C*H-C_6H_{11}), 1.17, 1.06, 0.97, 0.86 (2:2:2:2 ratio; OSi(*C*H$_3$)$_2$O); ^{29}Si NMR ([D]chloroform): δ = −71.08; −70.57; −69.31; −67.79 (2:1:2:1 ratio; O$_3$*Si*C_5H_9), −61.13 (*Si*-OH), −21.13 (2 Si; O{*Si*Me$_2$}$_4$O), −20.15 (2 Si; O{*Si*(CH$_3$)$_2$O}$_4$); IR: $\tilde{\nu}$ = 3626 (w), 2919 (s), 2848 (s), 1447 (m), 1259 (m), 1195 (m), 1076 (vs), 892 (m), 845 (m), 800 (s), 737 cm^{-1} (w); elemental analysis calcd for $C_{50}H_{102}O_{15}Si_{11}$ (1252.30): C 47.96, H 8.21; found C 47.97, H 8.02.

(*c*-C_5H_9)$_7$$Si_7O_9(OSiPh_2O)OH$ (7): A similar procedure as for compound **1** yielded **7** as a white micro crystalline material (81%). M.p. 248°C; ^{1}H NMR ([D]chloroform): δ = 7.82 (d, 2H; *o*-C*H*-C_6H_5), 7.61 (d, 2H; *o*-C*H*-C_6H_5), 7.49 (d, 4H; *m*-C*H*-C_6H_5), 7.36 (m, 2H; *p*-C*H*-C_6H_5), 2.39 (s, 1H; SiO*H*), 1.77 (m, 14H; C*H*$_2$-C_5H_9), 1.54 (m, 42H; C*H*$_2$-C_5H_9), 1.01 (m, 7H; C*H*-C_5H_9); ^{13}C NMR ([D]chloroform): δ = 135.85 (C_{ipso}-C_6H_5), 134.80 (C_{ipso}-C_6H_5), 134.29 (*o*-*C*H-C_6H_5), 133.83 (*o*-*C*H-C_6H_5), 130.45 (*p*-*C*H-C_6H_5), 129.92 (*p*-*C*H-C_6H_5), 128.05 (*m*-*C*H-C_6H_5), 127.63 (*m*-*C*H-C_6H_5), 27.48, 27.38, 27.26, 27.04, 26.98 (*C*H$_2$-C_5H_9), 22.85, 22.80, 22.78, 22.30, 22.26 (2:2:1:1:1 ratio; *C*H-C_5H_9); ^{29}Si NMR ([D]chloroform): δ = −46.69 (O*Si*(C_6H_5)$_2$O), −58.07 (*Si*OH), −65.17, −65.25, −66.21, −67.59 (1:1:2:2 ratio; O$_3$*Si*C_5H_9); IR: $\tilde{\nu}$ = 3636 (w), 2948 (m), 2864 (m), 1430 (w), 1246 (w), 1093 (s), 948 (w), 911 (w), 717 (m), 699 cm^{-1} (m); elemental analysis calcd for $C_{47}H_{74}O_{12}Si_8$ (1071.83): C 53.47, H 7.07, found C 53.33, H 6.85.

[(*c*-C_5H_9)$_7$$Si_7O_{10}(OSiMe_2O)(GaMe_2)]_2$ (8): A toluene solution of $GaMe_3$ (4.44 g, 0.39 mmol $GaMe_3$/g toluene; 1.73 mmol) was added to a cooled (−40°C) toluene (30 mL) solution of **1** (1.61 g, 1.73 mmol) and the mixture was allowed to warm to room temperature. The mixture was then stirred vigorously and heated to reflux until visual evolution of gas (measured using an oil bubbler) ceased. The mixture was subsequently stirred for 16 h at 60°C. The mixture was pumped to dryness and by adding hexanes (5 mL) and subsequent evaporation of the volatiles, final traces of toluene were removed. The product **8** was isolated in almost quantitative yield (1.75 g, 0.85 mmol, 98%). Analytically pure **8** was obtained by slow crystallization from hot methylcyclohexane (30 mL). M.p. 211°C; ^{1}H NMR ([D]chloroform, 50°C): δ = 2.01 (m, 28H; C*H*$_2$-C_5H_9), 1.70 (m, 56H; C*H*$_2$-C_5H_9), 1.48 (m, 28H; C*H*$_2$-C_5H_9), 1.21 (m, 14H; C*H*-C_5H_9), 0.53 (s, 6H; OSi(C*H*$_3$)$_2$O), 0.38 (s, 12H; GaC*H*$_3$), 0.36 (s, 6H; OSi(C*H*$_3$)$_2$O); ^{13}C NMR ([D]chloroform, 50°C): δ = 28.68, 28.10, 27.48, 27.28 (*C*H$_2$-C_5H_9), 25.56, 23.76, 23.51, 23.13, 22.95 (1:2:2:1:1 ratio; *C*H-C_5H_9), 1.28, 0.87 (OSi(*C*H$_3$)$_2$O), −2.49 (Ga(*C*H$_3$)$_2$); ^{29}Si NMR ([D]chloroform, 50°C): δ = −17.32 (O*Si*(CH$_3$)$_2$O), −59.47 (*Si*OGaMe$_2$), −64.38, −64.61, −65.99, −67.28 (1:1:2:2 ratio; O$_3$*Si*C_5H_9); elemental analysis calcd for $C_{78}H_{150}Ga_2O_{24}Si_{16}$ (2060.85): C 45.46, H 7.34; found C 45.54, H 7.40.

[(*c*-C_6H_{11})$_7$$Si_7O_{10}(O\{SiMe_2O\}_4)(GaMe_2)]_2$ (9): With the same procedure as for **8**, compound **9** was isolated in almost quantitative yield (98%). A sample suitable for elemental analysis was obtained by recrystallization of **9** from methylcyclohexane (30 mL) at −30°C. M.p. 207°C; ^{1}H NMR ([D]chloroform, 50°C): δ = 2.12 (m, 28H; C*H*$_2$-C_5H_9), 1.68 (m, 56H; C*H*$_2$-C_5H_9), 1.30 (m, 28H; C*H*$_2$-C_5H_9), 1.01 (m, 14H; C*H*-C_5H_9), 0.19–0.38 (s, 12H; GaC*H*$_3$), 0.19–0.38 (m, 48H; O{Si(C*H*$_3$)$_2$O}$_4$); ^{13}C NMR ([D]chloroform, 50°C): δ = 27.24–28.34 (*C*H$_2$-C_5H_9), 25.70, 25.55, 24.78, 24.70, 23.85 (2:1:1:2:1 ratio; *C*H-$\mathrm{C_5H_9}$), 1.17–1.49 (O{Si(*C*$\mathrm{H_3}$)$_2$O}$_4$), −0.56 (Ga(*C*$\mathrm{H_3}$)$_2$); ^{29}Si NMR ([D]chloroform, 50 °C): δ = −20.08, −20.92 (O{*Si*($\mathrm{CH_3}$)$_2$O}$_4$), −60.26 (*Si*-OGa$\mathrm{Me_2}$), −66.77, −68.27, −69.53, −70.39 (1:2:1:2 ratio; $\mathrm{O_3}$*Si*$\mathrm{C_5H_9}$); elemental analysis calcd for $\mathrm{C_{104}H_{214}Ga_2O_{30}Si_{22}}$ (2702.16): C 46.23, H 7.98; found C 46.06, H 8.05.

[(*c*-$\mathbf{C_5H_9}$)$_7$$\mathbf{Si_7O_{10}}$(OSi$\mathbf{Ph_2}$O)(Ga$\mathbf{Me_2}$)]$_2$ (10): By means of the same procedure as for **8**, compound **10** was isolated in almost quantitative yield (97 %). Suitable crystals for a single crystal X-ray diffraction study were obtained by recrystallization of **10** from hot methylcyclohexane (30 mL). Decomp. 229 °C; ^{1}H NMR ([D$_6$]benzene): δ = 8.03 (d, 4H; *o*-C*H*-$\mathrm{C_6H_5}$), 7.83 (d, 4H; *o*-C*H*-$\mathrm{C_6H_5}$), 7.42 (m, 8H; *m*-C*H*-$\mathrm{C_6H_5}$), 7.18 (m, 4H; *p*-C*H*-$\mathrm{C_6H_5}$), 1.92 (m, 28H; C*H*$_2$-$\mathrm{C_5H_9}$), 1.60 (m, 84H; C*H*$_2$-$\mathrm{C_5H_9}$), 1.08 (m, 14H; C*H*-$\mathrm{C_5H_9}$), 0.28 (s, 12H; GaC*H*$_3$); ^{13}C NMR ([D$_6$]benzene): δ = 152.55 (C_{ipso}-$\mathrm{C_6H_5}$), 149.66 (*o*-*C*H-$\mathrm{C_6H_5}$), 148.37 (*o*-*C*H-$\mathrm{C_6H_5}$), 135.08 (*p*-*C*H-$\mathrm{C_6H_5}$), 134.74 (*p*-*C*H-$\mathrm{C_6H_5}$), 127.93 (*m*-*C*H-$\mathrm{C_6H_5}$), 127.85 (*m*-*C*H-$\mathrm{C_6H_5}$), 28.49, 27.98, 27.39 (*C*$\mathrm{H_2}$-$\mathrm{C_5H_9}$), 25.14, 23.82, 23.67, 23.20, 23.06 (1:2:2:1:1 ratio; *C*H-$\mathrm{C_5H_9}$), −2.85 (Ga(*C*$\mathrm{H_3}$)$_2$); ^{29}Si NMR ([D$_6$]benzene): δ = −44.23 ($\mathrm{O_2SiPh_2}$), −59.07 (*Si*OGa$\mathrm{Me_2}$), −63.87, −64.11, −64.94, −66.65 (1:1:2:2 ratio; $\mathrm{O_3}$*Si*$\mathrm{C_5H_9}$); elemental analysis calcd for $\mathrm{C_{98}H_{158}Ga_2O_{24}Si_{16}}$ (2309.13): C 50.97, H 6.90; found C 50.39, H 6.90.

Cp″[(*c*-$\mathbf{C_5H_9}$)$_7$$\mathbf{Si_7O_{10}}$($\mathbf{O_2SiMe_2}$)]Ti($\mathbf{CH_2Ph}$)$_2$ (11): A solution of compound **1** (0.053 g, 50 µmol, 1.1 equiv) in [D$_6$]benzene (0.5 mL) was added to a solution of Cp″Ti($\mathrm{CH_2Ph}$)$_3$ (0.024 g, 45 µmol) in [D$_6$]benzene (0.5 mL), at room temperature. After 2 days at room temperature, NMR spectroscopy indicated that product **11** was formed quantitatively. ^{1}H NMR ([D$_6$]benzene): δ = 7.23 (s, 4H; $\mathrm{C_6H_5}$), 7.22 (s, 4H; $\mathrm{C_6H_5}$), 6.97 (m, 1H; $\mathrm{C_5}$*H*$_3$($\mathrm{SiMe_3}$)$_2$), 6.90 (m, 2H; $\mathrm{C_6H_5}$), 6.59 (m, 2H; $\mathrm{C_5}$*H*$_3$($\mathrm{SiMe_3}$)$_2$), 3.30 (d, $^2J_{\text{H-H}}$ = 9.9 Hz, 2H; C*H*$_2$Ph), 2.46 (d, $^2J_{\text{H-H}}$ = 9.9 Hz, 2H; C*H*$_2$Ph), 1.93 (m, 14H; C*H*$_2$–$\mathrm{C_5H_9}$), 1.69 (m, 28H; C*H*$_2$-$\mathrm{C_5H_9}$), 1.52 (m, 14H; C*H*$_2$-$\mathrm{C_5H_9}$), 1.21 (m, 7H; C*H*-$\mathrm{C_5H_9}$), 0.33 (s, 3H; OSi(C*H*$_3$)$_2$O), 0.27 (s, 18H; Si(C*H*$_3$)$_3$), 0.19 (s, 3H; OSi(C*H*$_3$)$_2$O); ^{13}C NMR ([D$_6$]benzene): δ = 150.01 (*ipso*-*C*$_6$$\mathrm{H_5}$), 133.95 (*C*$_5$$\mathrm{H_3}$($\mathrm{SiCH_3}$)$_2$), 131.24 (*C*$_5$$\mathrm{H_3}$($\mathrm{SiCH_3}$)$_2$), 128.51, 127.49, 125.69 (*C*$_6$$\mathrm{H_5}$), 122.82 (*C*$_5$$\mathrm{H_3}$($\mathrm{SiCH_3}$)$_2$), 85.42 ($^1J_{\text{C-H}}$ = 125 Hz; $\mathrm{CH_2Ph}$), 28.15, 27.40 (*C*$\mathrm{H_2}$-$\mathrm{C_5H_9}$), 25.58, 24.00, 23.81, 23.07 (1:2:2:2 ratio; *C*H-$\mathrm{C_5H_9}$), 1.38 (OSi(*C*$\mathrm{H_3}$)$_2$O), 0.69 (OSi(*C*$\mathrm{H_3}$)$_2$O), 0.44 (Si(*C*$\mathrm{H_3}$)$_3$); ^{29}Si NMR ([D$_6$]benzene): δ = −6.89 (*Si*($\mathrm{CH_3}$)$_3$), −16.43 (O*Si*($\mathrm{CH_3}$)$_2$O), −64.00, −64.08, −65.28, −66.45, −66.92 (1:1:2:1:2 ratio; $\mathrm{O_3}$*Si*$\mathrm{C_5H_9}$).

Cp″[(*c*-$\mathbf{C_6H_{11}}$)$_7$$\mathbf{Si_7O_{10}}$(O{$\mathbf{SiMe_2}$O}$_2$)]Ti($\mathbf{CH_2Ph}$)$_2$ (12): A solution of compound **4** (0.045 g, 50 µmol) in [D$_6$]benzene (0.5 mL) was added to a solution of Cp″Ti($\mathrm{CH_2Ph}$)$_3$ (0.024 g, 45 µmol, 1.1 equiv) in [D$_6$]benzene (0.5 mL) at room temperature. After 2 days at room temperature, NMR spectroscopy showed that product **12** was formed quantitatively. ^{1}H NMR ([D$_6$]benzene): δ = 7.26 (s, 4H; $\mathrm{C_6H_5}$), 7.25 (s, 4H; $\mathrm{C_6H_5}$), 7.06 (m, 1H; $\mathrm{C_5}$*H*$_3$($\mathrm{SiMe_3}$)$_2$), 6.91 (m, 2H; $\mathrm{C_6H_5}$), 6.56 (m, 2H; $\mathrm{C_5}$*H*$_3$($\mathrm{SiMe_3}$)$_2$), 3.46 (d, $^2J_{\text{H-H}}$ = 9.9 Hz, 2H; C*H*$_2$Ph), 2.39 (d, $^2J_{\text{H-H}}$ = 9.9 Hz, 2H; C*H*$_2$Ph), 1.65 (m, 42H; C*H*$_2$-$\mathrm{C_6H_{11}}$), 1.27 (m, 28H; C*H*$_2$-$\mathrm{C_6H_{11}}$), 1.03 (m, 7H; C*H*-$\mathrm{C_6H_{11}}$), 0.28 (s, 18H; Si(C*H*$_3$)$_3$), 0.22 (s, 6H; O{Si(C*H*$_3$)$_2$O}$_2$), 0.10 (s, 6H; O{Si(C*H*$_3$)$_2$O}$_2$); ^{13}C NMR ([D$_6$]benzene): δ = 149.96 (*ipso*-*C*$_6$$\mathrm{H_5}$), 137.82 (*C*$_5$$\mathrm{H_3}$($\mathrm{SiCH_3}$)$_2$), 133.84 (*C*$_5$$\mathrm{H_3}$($\mathrm{SiCH_3}$)$_2$), 133.02 (*C*$_5$$\mathrm{H_3}$($\mathrm{SiCH_3}$)$_2$), 128.29 (*C*$_6$$\mathrm{H_5}$), 127.61 (*C*$_6$$\mathrm{H_5}$), 125.18 (*C*$_6$$\mathrm{H_5}$), 122.82 (*C*$_6$$\mathrm{H_5}$), 85.76 ($^1J_{\text{C-H}}$ = 125 Hz; $\mathrm{CH_2Ph}$), 27.23–28.36 (*C*$\mathrm{H_2}$-$\mathrm{C_6H_{11}}$), 26.52, 25.70, 24.51, 23.88 (1:1:4:1 ratio; *C*H-$\mathrm{C_6H_{11}}$), 1.61, 1.25 (2:2 ratio; O{Si(*C*$\mathrm{H_3}$)$_2$O}$_2$), 0.55 (Si(*C*$\mathrm{H_3}$)$_3$); ^{29}Si NMR ([D$_6$]benzene): δ = −6.87 (*Si*($\mathrm{CH_3}$)$_3$), −20.31 (O{Si(*C*$\mathrm{H_3}$)$_2$O}$_2$), −66.86, −68.45, −68.99, −69.17, −69.57 (1:1:1:2:2 ratio; $\mathrm{O_3}$*Si*$\mathrm{C_5H_9}$).

NMR tube reactions of Cp″[(*c*-$\mathbf{C_5H_9}$)$_7$$\mathbf{Si_8O_{13}}$]Ti($\mathbf{CH_2Ph}$)$_2$, 11, and 12 with B($\mathbf{C_6F_5}$)$_3$: NMR tubes were charged with [D$_8$]toluene solutions of equimolar amounts (~75 µmol) of Cp″Ti($\mathrm{CH_2Ph}$)$_3$ and (*c*-$\mathrm{C_5H_9}$)$_7$$\mathrm{Si_8O_{12}}$(OH), **1**, or **4** and left for 24 h at 25 °C to form the corresponding titanium dibenzyl species (Cp″[(*c*-$\mathrm{C_5H_9}$)$_7$$\mathrm{Si_8O_{13}}$]Ti($\mathrm{CH_2Ph}$)$_2$, **11**, or **12** in situ. The solutions were cooled to −30 °C and [D$_8$]toluene solutions of B($\mathrm{C_6F_5}$)$_3$ were added. The NMR tubes were sealed with a Teflon tap and stored in liquid nitrogen before use. The formation of the ionic species was followed over time at 25 °C by ^{1}H and ^{19}F NMR spectroscopy.

Isoperibolic 1-hexene polymerizations: In the glove box, a vial (25 mL) was charged with 1-hexene (10 mL). To this the cocatalyst, either B($\mathrm{C_6F_5}$)$_3$ (40 µmol) or $[\mathrm{Ph_3C}]^+[\mathrm{B(C_6F_5)_4}]^-$ (11 µmol), was added as a toluene (0.5 mL) solution. The catalyst precursor, Cp″Ti($\mathrm{CH_2Ph}$)$_3$, Cp″[(*c*-$\mathrm{C_5H_9}$)$_7$$\mathrm{Si_8O_{13}}$]Ti($\mathrm{CH_2Ph}$)$_2$, **11**, or **12** (10 µmol), was then added as a toluene solution (0.5 mL). Whereas the B($\mathrm{C_6F_5}$)$_3$ activated system afforded a homogeneous reaction mixture, activation with $[\mathrm{Ph_3C}]^+[\mathrm{B(C_6F_5)_4}]^-$ resulted in precipitation of the active catalyst as a dark red oil that was suspended by stirring. The reaction mixtures were stirred for 6 ($[\mathrm{Ph_3C}]^+$ $[\mathrm{B(C_6F_5)_4}]^-$) or 24 h (B($\mathrm{C_6F_5}$)$_3$) and the temperatures of the reaction mixtures were monitored using a thermocouple inserted into the reaction vessel through a septum. The polymers were washed with ethanol and water to remove catalyst traces. Thorough drying yielded the polymer as a viscous oil. The polymers were identified by ^{1}H and ^{13}C NMR spectroscopy and GPC analysis.

DFT calculations: Standard computational methods based on density functional theory were employed by means of the Spartan program.[24] The functional used is the three-parameter exchange functional of Becke together with the correlation functional of Lee, Yang, and Parr (B3LYP).[25] For H, O, Si and Ti the basis sets used are the Pople-style basis sets 6-31G[26] with diffuse (+) s and p functions added on the heavy atoms and polarization function (d, p), adding one d function on the heavy atoms and one p function on the hydrogens (6-31+G-(d,p)).[27] The geometries of all the model compounds have been fully optimized using analytical gradient techniques at the B3LYP level of theory previously cited. No symmetry constraints have been introduced. The convergence criteria used in these calculations are 10^{-6} Hartrees for the energy, 4.5×10^{-4} Hartrees/bohr for the gradient, and 1.8×10^{-3} Å for the Cartesian coordinates.

X-ray crystal structure analyses of 10: A suitable crystal measuring (0.20 × 0.20 × 0.20 mm) was selected, mounted on a thin glass fiber using paraffin oil, and cooled to the data-collection temperature (203 K). Data were collected using 0.3° ω scans at 0, 90, and 180° in ϕ. Initial unit-cell parameters were determined from 60 data frames collected at different sections of the Ewald sphere. Semi-empirical absorption corrections based on equivalent reflections were applied.[28] Systematic absences in the diffraction data and unit-cell parameters were uniquely consistent with the reported space group. The structure was solved by direct methods, completed with difference Fourier syntheses, and refined with full-matrix least-squares procedures based on F^2. All hydrogen atoms were treated as idealized contributions. All scattering factors are contained in the SHELXTL 6.12 program library.[29] Bruker AXS SMART 1k CCD diffractometer, $\mathrm{Mo_{K\alpha}}$ radiation (λ = 0.71073 Å), T = 203(2) K, $0.20\times0.20\times0.20$ mm^3, $\mathrm{C_{98}H_{158}Ga_2O_{24}Si_{16}\cdot(C_7H_{14})}$ M_r = 2407.31, monoclinic, $P2_1/n$, a = 20.055(2), b = 16.0341(19), c = 20.913(3) Å, β = 95.106(2)°, V = 6698.3(14) Å^3, Z = 2, ρ_{calcd} = 1.194 g cm^{-3}, $\mu(\mathrm{Mo_{K\alpha}})$ = 0.605 mm^{-1}, total data = 46145, unique data = 11146, $wR(F^2)$ = 0.2256, $R(F)$ = 0.0815, GooF = 1.014, max. residual electron density 0.819 and −0.479 e Å^{-3}.

CCDC-232771 contains the supplementary crystallographic data for this paper. These data can be obtained free of charge via www.ccdc.cam.ac.uk/conts/retrieving.html (or from the Cambridge Crystallographic Data Centre, 12 Union Road,, Cambridge CB2 1EZ, UK; fax: (+44) 1223–336–033; or e-mail: deposit@ccdc.cam.ac.uk).

Acknowledgment

This work was financially supported by the Dutch Polymer Institute (R.D.) and the Spinoza grant awarded to R. A. van S.

---

[1] a) V. Ya. Davydov in *Adsorption on Silica Surfaces* (Ed.: E. Papirer), Marcel Dekker, New York, **2000**, pp. 63; b) N. R. E. N. Impens, P. van der Voort, E. F. Vansant, *Microporous Mesoporous Mater.* **1999**, *28*, 217.

[2] For example see: a) J. E. Mark, B. Erman, F. R. Eirich, *Science and Technology of Rubber*, 2nd ed., Academic Press, New York, **1994**, pp. 388; b) S. Schaal, A. Y. Coran, S. K. Mowdood, *Rubber Chem. Technol.* **2000**, *73*, 240.

[3] a) R. J. Gorte, *Catal. Lett.* **1999**, *62*, 1; b) J. H. Clark, *Acc. Chem. Res.* **2002**, *35*, 791.

[4] a) O. Olabisi, M. Atiqullah, W. Kaminsky, *Macromol. Chem. Phys.* **1997**, *37*, 519; b) G. G. Hlatky, *Chem. Rev.* **2000**, *100*, 1347; c) G. Fink, B. Steinmetz, J. Zechlin, C. Przybyla, B. Tesche, *Chem. Rev.*

2000, *100*, 1377; d) E. M. Carnahan, G. B. Jacobsen, *CATTECH* **2000**, *4*, 74.

[5] For example see: a) J. R. Park, T. Shiono, K. Soga, *Macromolecules* **1992**, *25*, 521; b) K. Soga, D. H. Lee, *Makromol. Chem.* **1992**, *193*, 1687; c) K. Soga, R. Koide, T. Uozumi, *Makromol. Chem. Rapid Commun.* **1993**, *14*, 511; d) J. Kratochvila, T. Shiono, K. Soga, *Makromol. Chem. Rapid Commun.* **1993**, *14*, 85; e) T. Uozumi, T. Toneri, K. Soga, *Macromol. Rapid Commun.* **1997**, *18*, 9; f) J. Xu, J. Zhao, Z. Fan, L. Feng, *Macromol. Rapid Commun.* **1997**, *18*, 875.

[6] a) M. Jezequel, V. Dufaud, M. J. Ruiz-Garcia, F. Carrillo-Hermosilla, U. Neugebauer, G. P. Niccolai, F. Lefebvre, F. Bayard, J. Corker, S. Fiddy, J. Evans, J.-P. Broyer, J. Malinge, J.-M. Basset, *J. Am. Chem. Soc.* **2001**, *123*, 3520; b) H. Ahn, C. P. Nicholas, T. J. Marks, *Organometallics* **2002**, *21*, 1788; c) C. P. Nicholas, H. Ahn, T. J. Marks, *J. Am. Chem. Soc.* **2003**, *125*, 4325.

[7] a) F. J. Feher, D. A. Newman, J. F. Walzer, *J. Am. Chem. Soc.* **1989**, *111*, 1741; b) F. J. Feher, D. A. Newman, *J. Am. Chem. Soc.* **1990**, *112*, 1931; c) F. J. Feher, T. A. Budzichowski, R. L. Blanski, K. J. Weller, J. W. Ziller, *Organometallics* **1991**, *10*, 2526; d) F. J. Feher, T. A. Budzichowski, K. Rahimian, J. W. Ziller, *J. Am. Chem. Soc.* **1992**, *114*, 3859; e) F. J. Feher, S. H. Philips, J. W. Ziller, *Chem. Commun.* **1997**, 829; f) R. Duchateau, H. C. L. Abbenhuis, R. A. van Santen, S. K.-H. Thiele, M. F. H. van Tol, *Organometallics* **1998**, *17*, 5222; g) T. W. Dijkstra, R. Duchateau, R. A. van Santen, A. Meetsma, G. P. A. Yap, *J. Am. Chem. Soc.* **2002**, *124*, 9856; h) T. W. Dijkstra, PhD thesis, Eindhoven University of Technology (The Netherlands), **2003**.

[8] R. Duchateau, *Chem. Rev.* **2002**, *102*, 3525, and references therein.

[9] a) R. Duchateau, R. J. Harmsen, H. C. L. Abbenhuis, R. A. van-Santen, A. Meetsma, S. K.-H. Thiele, M. Kranenburg, *Chem. Eur. J.* **1999**, *5*, 3130; b) F. T. Edelmann, Y. K. Gun'ko, S. Giessmann, F. Olbrich, *Inorg. Chem.* **1999**, *38*, 210; c) M. D. Skowronska-Ptasinska, R. Duchateau, R. A. van Santen, G. P. A. Yap, *Eur. J. Inorg. Chem.* **2001**, 133; d) J. R. Severn, R. Duchateau, R. A. van Santen, D. D. Ellis, A. L. Spek, G. P. A. Yap, *J. Chem. Soc. Dalton Trans.* **2003**, 2293.

[10] V. Lorenz, M. Spoida, A. Fischer, F. T. Edelmann, *J. Organomet. Chem.* **2001**, *625*, 1.

[11] a) R. M. Badger, S. H. Bauer, *J. Chem. Phys.* **1937**, *5*, 838; b) R. M. Badger, S. H. Bauer, *J. Chem. Phys.* **1940**, *8*, 288.

[12] S. Krijnen, R. J. Harmsen, H. C. L. Abbenhuis, J. H. C. van Hooff, R. A. van Santen, *Chem. Commun.* **1999**, 501.

[13] a) R. F. Cooksen, *Chem. Rev.* **1974**, *74*, 5; b) F. Bordwell, *Acc. Chem. Res.* **1988**, *21*, 456; c) A. Fachetti, Y.-J. Kim, A. J. Streitweiser, *J. Org. Chem.* **2000**, *65*, 4195; d) M. J. Kaufman, A. J. Streitweiser, *J. Am. Chem. Soc.* **1987**, *109*, 6097.

[14] a) A. Voigt, R. Murugavel, E. Parisini, H. W. Roesky, *Angew. Chem.* **1996**, *108*, 823; *Angew. Chem. Int. Ed. Engl.* **1996**, *35*, 748; b) F. J. Feher, T. A. Budzichowski, J. W. Ziller, *Inorg. Chem.* **1997**, *36*, 4082; c) R. Murugavel, M. G. Walawalkar, G. Prabusankar, P. Davis, *Organometallics* **2001**, *20*, 2639; d) M. Veith, H. Vogelgesang, V. Huch, *Organometallics* **2002**, *21*, 380; e) G. Gerritsen, R. Duchateau, R. A. van Santen, G. P. A. Yap, *Organometallics* **2003**, *22*, 100.

[15] For example see: a) R. Anulewicz-Ostrowska, S. Luliñski, J. Serwatowski, *Inorg. Chem.* **1999**, *38*, 3796; b) R. Anulewicz-Ostrowska, S. Luliñski, E. Pindelska, J. Serwatowski, *Inorg. Chem.* **2002**, *41*, 2525; c) E. Hecht, *Z. Anorg. Allg. Chem.* **2000**, *626*, 1642; d) S. Chitsaz, E. Iravani, B. Neumüller, *Z. Anorg. Allg. Chem.* **2002**, *628*, 2279.

[16] R. Duchateau, U. Cremer, R. J. Harmsen, S. I. Mohamud, H. C. L. Abbenhuis, R. A. van Santen, A. Meetsma, S. K.-H. Thiele, M. F. H. van Tol, M. Kranenburg, *Organometallics* **1999**, *18*, 5447.

[17] a) P.-J. Sinnema, K. Liekelema, O. K. B. Staal, B. Hessen, J. H. Teuben, *J. Mol. Catal.* **1998**, *128*, 143; b) F. Amor, A. Butt, K. E. du Plooy, T. P. Spaniol, J. Okuda, *Organometallics* **1998**, *17*, 5836.

[18] a) E. Y. X. Chen, T. J. Marks, *Chem. Rev.* **2000**, *100*, 1391; b) F. Song, R. D. Cannon, M. Bochmann, *Chem. Commun.* **2004**, 542.

[19] A. D. Horton, J. de With, A. J. van der Linden, H. van de Weg, *Organometallics* **1996**, *15*, 2672.

[20] For example see: a) X. Yang, C. L. Stern, T. J. Marks, *J. Am. Chem. Soc.* **1994**, *116*, 10015; b) R. Gomez, M. L. H. Green, J. L. Haggit, *J. Chem. Soc. Chem. Commun.* **1994**, 2607; c) M. L. H. Green, J. L. Haggit, C. P. Mehnert, *J. Chem. Soc. Chem. Commun.* **1995**, 1853; d) J. D. Scollard, D. H. McConville, S. J. Rettig, *Organometallics* **1997**, *16*, 1810; e) M. Bochmann, M. J. Sarsfield, *Organometallics* **1998**, *17*, 5908; f) G. J. Pindado, S. J. Lancaster, M. Thornton-Pett, M. Bochmann, *J. Am. Chem. Soc.* **1998**, *120*, 6816; g) D. A. Walker, T. J. Woodman, D. L. Hughes, M. Bochmann, *Organometallics* **2001**, *20*, 3772.

[21] S. J. Lancaster, O. B. Robinson, M. Bochmann, S. J. Coles, M. B. Hursthouse, *Organometallics* **1995**, *14*, 2456.

[22] a) A. G. Massey, A. J. Park, *J. Organomet. Chem.* **1964**, *2*, 245; b) A. G. Massey, A. J. Park, *J. Organomet. Chem.* **1966**, *5*, 218.

[23] J. C. W. Chien, W.-M. Tsai, M. D. Rausch, *J. Am. Chem. Soc.* **1991**, *113*, 8570.

[24] R. G. Parr, W. Yang in *Density Functional Theory of Atoms and Molecules* (Eds.: R. G. Parr, W. Yang), Oxford Science Publications, Oxford, **1989**.

[25] a) A. D. Becke, *J. Chem. Phys.* **1993**, *98*, 5648; b) C. Lee, W. Yang, R. G. Parr, *Phys. Rev. B* **1988**, *37*, 785.

[26] W. J. Hehre, L. Radom, P. V. R. Schleyer, J. A. Pople, *Ab Initio Molecular Orbital Theory*, Wiley, New York, **1986**.

[27] a) M. J. Frisch, J. A. Pople, J. S. Binkley, *J. Chem. Phys.* **1984**, *80*, 3265; b) R. Krisnan, J. S. Binkley, R. Seeger, J. A. Pople, *J. Chem. Phys.* **1980**, *72*, 650.

[28] R. Blessing, *Acta Crystallogr. Sect. A* **1995**, *51*, 33.

[29] G. M. Sheldrick, Bruker AXS, Madison, WI, **2001**.

Received: March 2, 2004